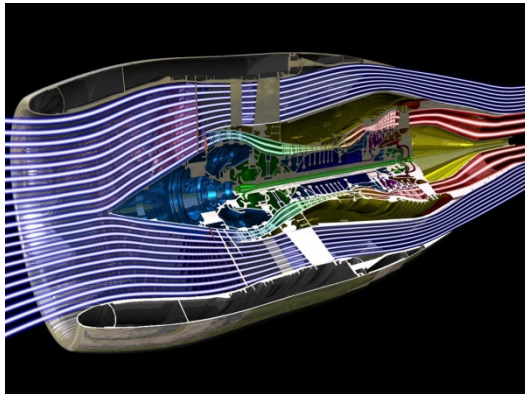




University of Beira Interior  
Aerospace Sciences Department



# Experimental Study on the Mixing of Confined Coaxial Jets



Joel Nogueira Fonseca

Covilhã

June 2009

Joel Nogueira Fonseca

# Experimental Study on the Mixing of Confined Coaxial Jets

Dissertation submitted to the University of Beira Interior for the Master  
Degree in Aeronautical Engineering

Thesis realized by supervising of Prof. Dr. André Resende Rodrigues Silva

Covilhã, June 2009

*Dedicated To My Parents*

## Resumo

A mistura turbulenta de jactos coaxiais confinados é um complexo processo dinâmico com muitas aplicações práticas, como em ejectores, bombas a jacto, queimadores industriais, câmaras de combustão de motores a jacto, foguetes nucleares gasosos, câmaras de mistura, afterburners<sup>1</sup>, motores turbofan. Nestas últimas aplicações, o confinamento é também de interesse fundamental, porque envolve certos fenómenos de interacção de escoamentos turbulentos, cujos detalhes não estão ainda quantitativamente completamente entendidos.

Os parâmetros que estão envolvidos no processo de mistura e que são os principais responsáveis pela complexidade do processo são ambos parâmetros geométricos ou parâmetros operacionais tais como: razões de velocidade, temperatura ou densidade, níveis de turbulência dos jactos, gradientes de pressão, interacção entre as paredes e os jactos ou a relação entre os diâmetros das condutas e mistura do jacto interno. Na literatura, existe alguns estudos que relatam a influência de alguns parâmetros geométricos e operacionais no processo de mistura turbulenta.

A mistura turbulenta de dois jactos paralelos é afectada pelo confinamento, velocidade, e intensidade de turbulência. O objectivo deste trabalho é estudar o efeito dos níveis iniciais de turbulência de cada jacto coaxial no processo de mistura turbulenta com razões de diâmetro inferior a 2, que é o caso de motores turbofan de baixo bypass. A utilização de razões de intensidade de turbulência convenientes entre o jacto interior e o exterior deve ser um instrumento mais eficaz para controlar a mistura turbulenta entre o fluxo interior e o exterior ( $\theta$ ). O objectivo do presente trabalho é estudar o efeito de ( $\theta$ ) no desenvolvimento do jacto e identificar os regimes associados, em especial a produção de uma zona de recirculação na zona central perto da saída dos jactos. Para isolar os efeitos das características radiais cilíndricas, foi adoptado uma configuração de geometria bidimensional. Os resultados foram obtidos para uma razão de velocidades,  $\lambda$ , de 2, com intensidades de turbulência próxima dos 30% da velocidade média do fluxo mássico ( $U_{\text{mean}}$ ) que corresponde a uma razão de intensidades de turbulência de  $\theta=1.5$ . Antes das medições de velocidades no escoamento, foi realizada a visualização para dar uma imagem qualitativa do escoamento para orientar a escolha dos locais de medição.

## Abstract

The turbulent mixing of coaxial confined jets is a complex dynamic process that is applied in a large number of devices such as the engineering ejectors, pumps jet, industrial burners, combustion chambers of jet engines, nuclear rockets gas, mixing chambers of turbofans, afterburners, and so on. The study of the aerodynamic performance of coaxial jets in different types of confinement also has a fundamental interest because it involves the interaction of different turbulent flow phenomena, whose details are not yet very well known quantitatively. The parameters that are involved in the process of mixing and are primarily responsible for the complexity of the process are both geometric or operational parameters such as: velocity, temperature or density ratios, compressibility effects, levels of turbulence of jets, pressure gradient, interaction between the walls and the jets or the ratio between the diameters of the mixing duct and the internal jet nozzle. In the literature several studies report the influence of some geometrical parameters and operating in the process of turbulent mixing.

Turbulent mixing of two parallel streams is affected by confinement, velocity ratio, and turbulent intensity. The objective of this work is to study the effect of the initial levels of turbulence of each coaxial jet in the process of turbulent mixing for diameter ratios less than 2, which is the case of very low bypass turbofan engines. The use of convenient turbulent intensity ratios between the inner and the outer flow should be a most effective tool to control the turbulent mixing between the inner and outer flow ( $\theta$ ). The aim of the present work is to study the effect of  $\theta$  on the flow development and to identify the associated regimes, and in particular the production of a flow reversal in the central zone near the jets exit. To isolate the characteristic radial effects of a cylindrical geometry a bi-dimensional configurations was adopted. The present results were obtained for a velocity ratio,  $\lambda$ , of 2, and turbulent intensities of 30% the mean mass flow velocity ( $U_{\text{mean}}$ ) that correspond to a ratio between the outer and inner jets of  $\theta=1.5$ . Prior to the measurements flow visualization was performed to give a qualitative picture of the flow and to guide the choice of the measurement locations.

## Acknowledgements

I would like to express my gratitude to my supervisor, Professor André Resende Rodrigues Silva, for his guidance, advices and the total availability to support my work

I would also like to thank Prof. Dr. Jorge Manuel Martins Barata for the knowledge transmission and support during this work.

I 'am grateful for the support of the Aerospace Science Department of University of Beira Interior, and especially to all my friends of the Astronautics and Aeronautics Research Center, AeroG.

I want to thank my parents that work hard to allow me to study and support me in every decision and step throughout my years as a student.

Joel Fonseca,  
Covilhã 2009

# INDEX

Resumo .....	iv
Abstract.....	v
Acknowledgements .....	vi
Index of Figures.....	ix
Index of Tables .....	ix
Nomenclature.....	x
CHAPTER 1 .....	1
1 Introduction .....	1
1.1 Introduction .....	1
1.2 Background.....	1
1.3 Motivation .....	12
CHAPTER 2 .....	14
2 Experimental Method .....	14
2.1 Introduction .....	14
2.2 Description of the Wind Tunnel Design.....	14
2.3 Description of the method .....	19
2.3.1 Principles of LDA.....	19
2.3.2 Seeding .....	24
2.4 Alignment and Calibration of the Experimental Setup .....	25
2.5 Measurements.....	26
CHAPTER 3 .....	27
3 Results .....	27
3.1 Introduction .....	27
3.2 Visualization.....	27

## INDEX

---

3.3 Vertical Profiles:.....	29
3.4 FlowField.....	36
3.5 Relations with the Shear layer.....	40
CHAPTER 4.....	42
4 Conclusions.....	42
References: .....	A



## Index of Figures

Fig. 1 Initial Region of Co-axial, Confined Jets .....	2
Fig. 2 Mean Field Concentration ( $\lambda=2$ ) and instantaneous picture of the flow ( $\lambda=3$ ) [27] .....	7
Fig. 3 Schema of a turbofan engine.....	13
Fig. 4 Experimental Method .....	14
Fig. 6 Draw of the Designed Wind Tunnel for $\lambda=6$ .....	16
Fig. 5 Schema of the Designed Wind Tunnel .....	16
Fig. 7 Picture of part of the Wind Tunnel with details of the convergent and divergent.....	17
Fig. 8 Wind Tunnel and Test Section.....	18
Fig. 9 Light Scatter from a moving seeding particle .....	19
Fig. 10 Scattering of two incoming laser beams.....	20
Fig. 11 Fringes form where two coherent laser beams cross .....	21
Fig. 12 Diagram of the Experimental Setup with Laser .....	22
Fig. 13 Traverse System with the transmitting/receiving Optics System.....	23
Fig. 14 Software BSA FLOW .....	24
Fig. 15 Seeding machine .....	25
Fig. 16 Schema of the Experimental Setup .....	28
Fig. 17 Mean Flow Concentration for $\lambda=2$ .....	28
Fig. 18 Complete Vertical Profile of $U_{mean}$ for the first station .....	30
Fig. 19 Vertical Profiles of Mean Velocities Characteristics $U/U_{med}$ .....	31
Fig. 20 Vertical Profiles of mean velocities characteristics $V/U_{med}$ .....	33
Fig. 21 Vertical Profiles of fluctuating velocities $u'_{RMS}/U_{med}$ .....	34
Fig. 22 Vertical Profiles of fluctuating velocities $v'_{RMS}/U_{med}$ .....	35
Fig. 23 Isolines of mean velocity characteristics $U/U_{med}$ .....	36
Fig. 24 Isolines of mean velocity characteristics $V/U_{med}$ .....	37
Fig. 25 Isolines of turbulent characteristics $u'_{RMS}/U_{med}$ .....	38
Fig. 26 Isolines of mean velocity characteristics $v'_{RMS}/U_{med}$ .....	38
Fig. 27 Spreading rate of the outer flow.....	40
Fig. 28 Variation of the location of the shear layer interface with distance to the jets exit.....	40
Fig. 29 Variation of the mean horizontal velocity component of the shear layer.....	41

## Index of Tables

Table 1 Dimensions of the Wind Tunnel Adaption for $\lambda=1.5, 3, 6$ and $10$ . .....	16
Table 2 Characteristics of Dantec LDV Flowlite 2D.....	23

## Nomenclature

$D_i$	= Diameter of the inner jet
$D_o$	= Diameter of the outer jet
$U_i$	= Horizontal Velocity of the inner jet
$U_o$	= Horizontal Velocity of the outer jet
$\rho_i$	= Density of the inner jet
$\rho_o$	= Density of the outer jet
$\lambda$	= Velocity Ratio ( $\lambda=U_o/ U_i$ )
$\lambda_c$	= Critical Velocity Ratio
$U_{med}$	= Mean Velocity
$U_{mean}$	= Horizontal Mean Velocity
$V_{mean}$	= Vertical Mean Velocity
$u_{RMS}$	= Horizontal Fluctuation of the Horizontal Mean Velocity
$v_{RMS}$	= Vertical Fluctuation of the Vertical Mean Velocity
$M$	= Momentum Flux
$\theta_{01}$	= Momentum Thickness of the inner Jet
$\theta_{02}$	= Momentum Thickness of the outer Jet
$A_i$	= Area of the exit of the inner jet
$A_o$	= Area of the exit of the outer jet
$\nu$	= Kinematic Viscosity
$\theta$	= Turbulence Intensities Ratio

# CHAPTER 1

## 1 Introduction

### *1.1 Introduction*

Turbulent mixing of confined co-axial jets is a complex dynamic process which finds application in a number of engineering devices such as ejectors, jet pumps, industrial burners, jet engine combustion chambers, gaseous nuclear rockets, turbofan engine mixing chambers, afterburners, etc. The Study of the aerodynamic behavior of co-axial jets in different types of confinement is also of basic interest because it involves a certain interacting turbulent flow phenomena, the details of which are not yet fully understood quantitatively.

### *1.2 Background*

Coaxial jets are composed of an inner jet issued from a nozzle of diameter  $D_i$  and an outer annular jet issued from an outer annulus of diameter  $D_o$  ( $D_o > D_i$ ).  $U_o$  and  $U_i$  designate the respective velocities of the inner and outer jets. One of the important parameters characterizing the coaxial jet dynamics is the ratio between the outer to the inner jet momentum flux,  $M = \rho_o U_o^2 / \rho_i U_i^2$  where  $\rho_1$  and  $\rho_2$  are, respectively, the inner and outer density. For constant density jets ( $\rho_o = \rho_i$ ), the momentum flux ratio reduces to the velocity ratio  $\lambda = U_o / U_i$ .

These jets are situated in-between two limiting cases: a single round jet ( $\lambda = 1$ ) and a purely annular jet ( $\lambda \rightarrow \infty$ ). Purely annular jets are characterized by the presence of a big recirculation bubble near the jet axis. Since this backflow is absent for small enough values of  $\lambda$ , there exists a critical velocity ratio  $\lambda_c$  which separates the two different main flow regimes, without recirculation bubble for  $1 < \lambda < \lambda_c$  and with recirculation bubble for  $\lambda > \lambda_c$ .

The factors that are involved in a mixing process and are also primarily responsible for the complexity are: the velocity ratio, temperature ratio, density ratio, compressibility and turbulence levels of the two streams, swirl, pressure gradient, interaction between wall bounded and free shear flows, mixing duct to inner jet nozzle diameter ratio, and thickness of the inner duct wall [2-6].

The complex nature of the near field structure of a ducted co-axial jets configuration can be appreciated from Fig. 1, which refers to a typical condition with comparable inner and outer jet areas. The flow field that arises from the interaction of co-axial jets and their mixing can be considered to comprise of three main zones of flow development as shown in the figure. Zone I is the initial merging zone wherein the core and the annular streams enter the mixing duct with different uniform axial velocities. The initial zone consists of two different potential

flow regions, A and B, and two different shear flow regions, i.e. the jet shear and the boundary layer regions, C and D, respectively. The shear regions increase in size and the potential flow regions decrease in size in the flow direction. The annular stream potential core disappears when the shear region and the wall boundary layer meet.

Zone II is the intermediate merging zone, where the largest momentum exchange between the jets takes place. The central potential flow region no longer exists in this zone for  $\lambda > 1$ , while for  $\lambda < 1$ ; it exists but continues to decrease.

Zone III is the fully merged zone, in which the flow conditions become progressively similar to those of a single jet [2, 3]. Further downstream, flow becomes fully developed

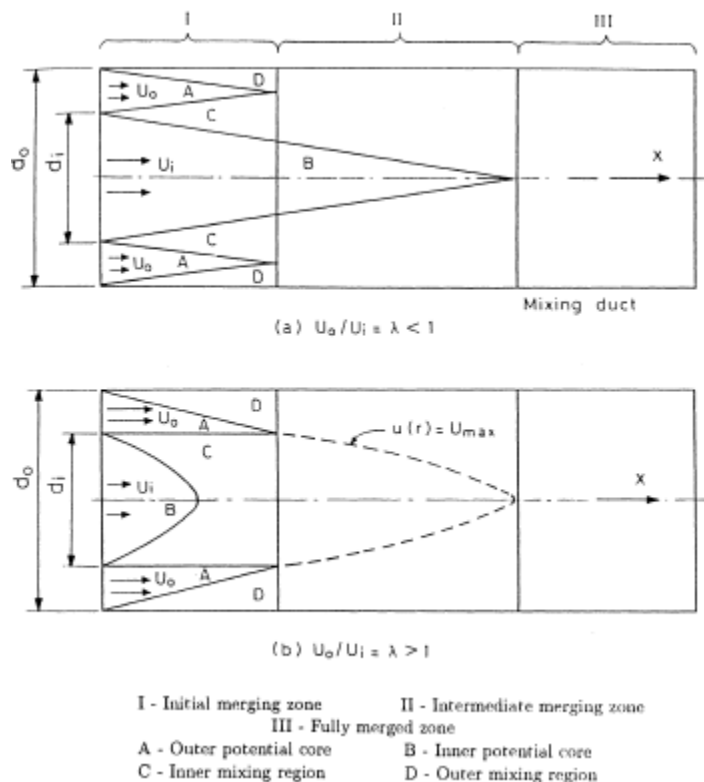


**Fig. 1 Initial Region of Co-axial, Confined Jets**

and self-similar (a similarity exists between velocity profiles at each cross-section along the streamwise axis) and a boundary layer type analysis usually fits the experimental data well.

The simplified picture of the complex flow presented above is further complicated by the presence of boundary layers on both the surfaces of the inner duct wall (splitter plate) and the subsequent annular wake trailing from the inner duct into the initial merging zone. The initial jet spreading rate and the length of zone I are sensitive to the inner duct (nozzle) geometry and the inlet flow conditions; vortex shedding from thick nozzle wall may accelerate the erosion of the potential core and enhance mixing with the entrained stream [6].

Acharya [3] was the first to make a review of all the works carried out on jet-mixing studies which dated back from 1864 to 1951. However, none of the studies conducted during that period was on confined jets. Acharya [3] was the first to make a detailed investigation to study the influence of velocity and temperature ratios on the mixing process of confined jets. The work that has been done on confined jet mixing since then, has definitely contributed to the understanding of the complex process of turbulent mixing. There is an initial region where the inner fluid decelerates, before being accelerated by the annular flow.

However, a survey of the literature indicates that there still exist some areas of ducted mixing where little attention has been focused [7]. As mentioned above, Acharya [3] made a detailed investigation on effect of velocity ratio of the two streams on the turbulent mixing process. He studied the turbulent mixing of co-axial jets both theoretically and experimentally and concluded that the turbulent friction between the two streams is larger in confined jets than in unconfined jets and that the absolute value of the difference of velocities between the two streams considerably influenced the mixing between the two jets by enhancing the momentum transfer between them.

Experiments conducted by Zawacki and Weinstein [8] and Rozenman and Weinstein [9] over a wide range of velocity ratios showed the presence of a circulating vortex at high velocity ratios to which they attributed the enhanced mixing between the two streams. The experimental results for  $\lambda < 1$  also showed that uniformity in velocity profile is achieved much faster for higher velocity ratio [2-5]. A wide range of velocity ratios,

thus covered by researchers, clearly shows that the velocity ratio has a very strong influence on turbulent mixing process. The rate of momentum transfer between the jets increases as the velocity ratio is increased, promoting faster mixing.

Durao and Whitelaw [10] used a Pitot tube, a Preston tube, normal and 45° hot wire probes to investigate the developing region of coaxial jets at downstream distances up to 17 outer diameters. The initial condition corresponds to fully developed pipe and annulus flows with a significant separation between the two. Their measurements were obtained for two velocity ratios  $U_i/U_o$  of 0.62 and 0.23 which means that the inner jet is completely stopped. Their results showed that coaxial jets tend to reach a self-preserving state much more rapidly than axisymmetric single jets. The attainment of the fully developed state is a function of the velocity ratio ( $U_i/U_o$ ) and zero velocity ratio leads to the most rapid development. Also their experiments showed that the flow possesses locations of zero mean-velocity gradient which are not coincident with locations of zero shear stress.

For three velocity ratios of 2.5, 1.67 and 1.15 and using a hot wire anemometer Ko and Au [11] made measurements in the initial region of coaxial jets. The mean velocity measurements within the initial region of coaxial jets of high mean-velocity ratio ( $U_i/U_o > 1$ ) isolate three separate zones as in cases of mean-velocity ratio less than unity: the initial merging, the intermediate and the fully merged zone. Similarity of the mean velocity profiles is obtained in each of the three zones isolated. The similarity found applies not only to the outer mixing region but also in inner mixing region inside the jet, and agrees well with the single jet results. Except for the inner mixing region, similarity of the turbulence intensity profiles is also obtained in the whole jet and also agrees well with single jet results.

Warda et al.[12], investigated experimentally the influence of the magnitude of two initial velocities for a coaxial jet. Not only the velocity ratio,  $\lambda$ , affects the evolution and the structure of coaxial jets but also the absolute values of the velocity of each stream, particularly in the region  $10 < x/D < 20$ . The reduction in the absolute values of the velocities of both streams while keeping the same velocity ratio,  $\lambda$  constant made the jet decay faster along the centerline. For the same velocity ratio, when the velocity of each

stream (inner and outer) was reduced, the growth of the half width of coaxial jets with  $\lambda > 1$  was increased.

Studies on effect of turbulence level [13, 14] showed that a higher turbulence level favors faster mixing. A similar observation was made regarding the effect of swirl on the process of turbulent mixing [15, 16].

Using laser Doppler anemometry (LDA) Buresti et al. and Warda et al. [17–18] proposed a significant data base for a particular coaxial jet configuration. This base provides mean axial velocities profiles, turbulence intensities and shearing tensions in initial and intermediate regions. These authors took typical turbulence characteristics of industrial applications such as premixed burners. They specified that quantities defining the configuration, and influencing potentially the characteristics of the three regions of a coaxial jet are numerous: the inner and outer velocity ejection, the inner and annular surfaces, the inner nozzle wall thickness, the importance of the boundary layer thicknesses at the exit, as well as their state (laminar or turbulent), and the turbulence levels at the nozzle exit.

A wide range of diameter ratios (2-38) is covered by previous published work simulating various applications [7]. It was found that when the diameter ratio is high, the momentum transfer between the jets will increase when  $\lambda > 1$  and the uniformity of the velocity profile is achieved much faster. On the other hand, when the diameter ratio is small, the momentum transfer between the jets increases when the velocity ratio,  $\lambda$ , is less than 1. Razinsky and Brighton [1] studied the effect of diameter ratio by varying the diameter ratio of the jets from 3 to 6. They found slightly higher levels of turbulence when the diameter ratio is increased; however, the length required for complete mixing was not affected much in the range of diameter ratios studied. Studies on the effect of the diameter ratio with reference to application in ejectors have shown that entrainment of the secondary stream increases linearly with diameter ratio [19].

Matsumoto et al. [20] performed experimental studies on influence of nozzle conditions such as thickness of nozzle walls or boundary layers on the inside and outside walls of the nozzle on the characteristics of jets in the main region at four different velocity ratios ranging from 0.24 to 0.82. They found that for small values of  $k$ , the velocity decay on the central axis and the intensity of turbulence are hardly affected by the wall

thickness, while for large values of  $\lambda$ , the tendency of velocity decay becomes remarkable and the turbulence intensity is affected heavily by the wake behind the nozzle wall with an increase in the wall thickness.

Dziomba and Fiedler [21], studying the influence of the initial conditions on the development of two-dimensional mixing- layers, showed that when the thickness of the splitter plate separating two streams of different velocity is increased, the Kelvin-Helmholtz instability of the shear layer is progressively replaced by a regular alternate shedding of vortices in the wake.

Nikitopoulos et al.[22] compared non forced flows in axisymmetric coaxial nozzles and square nozzles with initial turbulent levels. Through visualization and local measurements of velocity, they found a slight increase on the mixing on square nozzles compared with the coaxial nozzles, given to the different initial velocity profiles between the configurations.

Bitting et al, [23] with measurements and visualizations by DPIV, compared flows on axisymmetric coaxial nozzles and square nozzles observing a greater transfer of momentum in squared jets than in coaxial jets. They viewed that the non mixed internal region decreases with the decrease of velocity ratio and also viewed instable recirculation and reversal flow phenomena at the end of the internal core of the jet for low velocity ratios.

Balarac and Si-Ameur [24] through numerical simulation associated with the mixing process of axisymmetric coaxial jets verified that the mixing process shows an intermittent character as a result of fluid injections caused by counter-rotating vortices along the flow.

Villermaux, [25] studied the effects on mixing in a confined turbulent flow of a low density jet with low velocity in the inner ring with a jet of high speed on the annular ring. He concluded that the overall relationship between the slow dense jet and the outer jet, and also the formation of drops in gas-liquid coaxial jets can be perceived by the instability of shear stress between the phases.

It is shown that the shape of the profile of velocities in the outer ring of the injector, and the thickness of vorticity influences the growth rate of the instability. When the ratio of



moments (energy) between the phases is above  $M > 35$ , a transition occurs for a recirculation flow, the efficiency of the properties of the mixture is quantified.

In an experimental study of two mixtures of confined coaxial jets by Zhdanov et al. [26], in an investigated distance between  $0.1 \leq x/D \leq 9.1$ , the mean velocity field has no time to form, is disturbed. Only when the recirculation zone is formed, the mean velocity field, is defined over the range investigated. The scalar field takes place in front of velocity. Since the scalar transfer is determined by the dynamics of the flow, the development of the scalar field of the jet is attributed to the influence of unstable vortices creating a mixing layer during the scalar transfer.

Rehab, Villermaux, and Hopfinger [27] experimentally showed that the coaxial jet dynamics and its vortex topology are strongly dependent on the shape of the inlet nozzle. Indeed, different shapes lead to significant variations of the two shear layers which are present in the coaxial jet: the inner shear layer at the interface between the inner and the outer jets and the outer shear layer on the external border of the outer jet.

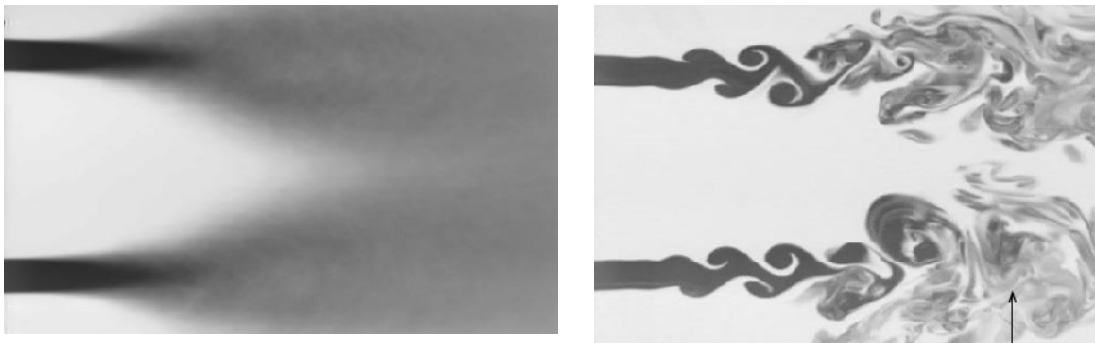


**Fig. 2 Mean Field Concentration ( $\lambda=2$ ) and instantaneous picture of the flow ( $\lambda=3$ ) [27]**

Above a critical velocity ratio  $\lambda_c$ , the inner potential cone is truncated by a reverse flow and a wake-type regime is active. This new flow pattern is characterized by the existence of an unsteady recirculation bubble. The transition mechanism to a wake regime is explained by a simple model which predicts satisfactorily  $\lambda_c$ . The size of the recirculating bubble increases with  $\lambda$  and reaches a maximum length for  $\lambda = 1$ , typically equal to one inner jet diameter  $D_i$ . The mean reverse flow velocity is proportional to  $U_o$ .

Velocity and mean static pressure measurements confirm our reasoning concerning the two flow regimes and the transition to a recirculating flow.

According to Revuelta [28], in the development of the jet and also in the region of recirculation flow, the approximation of the boundary layer can be used to describe the flow, whereas the Navier-Stokes equations are necessary to describe the outside region around the jet and the final phase of transition.

Talamelli and Gavarini [29] by visualizations shows the presence of an alternate vortex shedding behind the inner duct wall separating the two jets, This phenomenon is present for a specific range of velocity ratios and for finite thickness of the duct wall, and may be related to the onset of a self-excited temporally growing global wake instability. The spatial stability analysis shows that in the wake. Close to the jet exit, the most unstable mode is the jet mode characterized by an unison displacement of the critical layers. In this region the azimuthal wave number does not seem to influence the stability characteristics of the jet. The results show that with sufficiently low wake velocities this mode may become locally absolutely unstable. The shear-layers thicknesses change the extension of the region where the flow remains absolutely unstable, affecting also the absolute growth rate of the instability.

Dahm and Dimotakis [30], using LIF techniques (Laser-induced fluorescence), viewed free jet entrainment and mixing in water. The results showed a quantitative assessment in the presence of an organization of large-scale mixing, similar to turbulent jets. The instantaneous composition of the mixed fluid along the jet is approximately uniform in large regions, but has areas of non-mixing along the jet. The probability of finding fluid outside the jet increases at regular intervals, with a tendency to periodicity. By increasing the Reynolds number, decreases the probability of finding fluid outside the jet.

Recently, Ahmed and Sharma [31] presented a detailed review of work in this field and, moreover, with measurements by LDV and readings of static and total, presented seven velocities ratio, the velocities profiles, turbulence intensities, distributions of mean velocity and total pressure drop due to the process of turbulent mixing in a coaxial configuration and confined axisymmetric low rate of "bypass". Concluded that the process of turbulent mixing depends strongly on the velocity ratio between the two jets.

They found that the drop in total pressure is bigger when the velocity gradient between the jet increases, while for velocity ratios close to 1, the pressure drop is minimal.

Champagne and Wygnanski [32] were the first who used a hot wire anemometer in their turbulent coaxial jets research. Their observations were made for two nozzles surfaces ratios of 0.94 and 1.28 and for various velocities ratios ranging between 0 and 10. Champagne and Wygnanski showed that jet half thickness growth is not very sensitive to velocities change and nozzles surfaces ratios. They also proved that the external potential cone length seems to be independent of velocities ratios and equal to eight times the annular tube thickness. However, the inner potential cone length is strongly dependent on velocities and nozzles surfaces ratios. These effects are more noticed when external velocity is larger than interior velocity.

Ribeiro et al. [33, 34] reported using hot-wire anemometry, values of mean velocity, Reynolds stresses and probability density distribution of fluctuating velocity for the axisymmetric turbulent coaxial jets, with and without swirl. The results proved that, for velocities ratios ranging between 0.65 and 1.5, the non-swirling coaxial flow configurations reached the self-similar state within a much smaller distance than that of the round free jet. This is due to the mixing layer and vortex shedding that occurs in the region downstream the separation wall between the two streams. In the presence of swirl, the coaxial jet is developing it-self faster.

Dahm *et al.*[35] performed comprehensive flow visualizations of the vortex patterns and dynamics of their interactions in the near field of a round coaxial jet. They state that between each pair of streams, there is a velocity jump resulting from the difference in stream velocities together with a velocity defect imparted by the viscous boundary layers on either side of each nozzle lip. It is useful to conceptually view this compound velocity profile as being composed of a wake component and a shear layer component resulting, respectively, from the symmetric and antisymmetric parts of profile. Dahm *et al.* conclude that even over the limited range of parameters considered, a wide variety of dramatically differing near field vortex patterns can arise. These different patterns result in very different interaction dynamics that can depend both on the velocity ratio and on the absolute velocities of the two coaxial streams. The changes in potential core length also depend strongly on the differing near field vorticity dynamics. These variations in

core length are not simply, or even monotonically, dependent on the velocity ratio of the two jets, as was suggested previously, but instead show a nonlinear dependence.

Sadr and Klewicki [36] studies the near-field region of a coaxial jet flow for  $Di / Do = 0.39$  and for  $\lambda = 1.11, 0.8, 0.48,$  and  $0.18$  using molecular tagging velocimetry.

In the region very close to the jet exit the profiles of axial intensity and velocity gradient intensity support earlier results, indicating the existence of two trains of vortices shed from the two sides of inner jet wall. The magnitude of these intensities on each side of the inner jet wall depends on the absolute velocity of the corresponding jet. For the velocity ratios examined here, the two trains of vortices are most likely engulfed and annihilated within the larger mixing layer between the two jets before  $x/Di=2$ . The wake component of the inner mixing region was identifiable at all  $h$ . Its magnitude and extent, however, depends on  $\lambda$ . The calculated shear stress combined with the gradient of the mean velocity indicates that the turbulent characteristics of the flow in a coaxial jet are a function of  $\lambda$  for both the inner and outer shear layers. This is in agreement with the results of the axial intensity measurements suggesting that the rate of increase of turbulence intensity in each shear layer depends on the velocity ratio for that shear layer.

Lima and Palma [37], studied experimentally with Laser Doppler Anemometry the mixing of coaxial jets in a confined cylindrical duct. The location of the minimum velocity has been used as an indicator of the end of the inner potential core. The end of the inner potential core is also the end of the so-called initial merging zone or identically the end of entrainment of the inner jet by the co-flowing annular flow. The occurrence of the backflow region agreed with previous studies in non-confined flows and apparently, the confinement played no role in the onset of a region with axial negative velocity. In case of backflow, axial turbulence intensity exhibited 2 peak values, at the location where the axial velocity reached its minimum and where the longitudinal gradient of axial velocity was larger. The increase in mean axial velocity causes the decrease of mean concentration at the flow axis, with the instantaneous concentration fluctuation maximum being observed at the same longitudinal position where mean axial velocity was minimum. Radial turbulent mass transport was in accordance with gradient-transport methods; however, counter-gradient axial mass

transport prevailed in the flow inner region of the flow, after the disappearance of the inner core.

Balarac & Métais [38], by direct numerical simulation, characterize the respective thicknesses of the inner and outer shear layers by their momentum thicknesses  $\theta_{01}$  and  $\theta_{02}$ . They investigate the influence of  $\theta_{01}$  on the transitional processes in the jet near field. For  $\lambda < \lambda_c$  and for  $\lambda > \lambda_c$ , small values of  $\theta_{01}$  were associated with an earlier jet transition to turbulence due to a faster destabilization of the inner shear layer. For  $\lambda < \lambda_c$ , they showed that the three dimensionality of the primary jet vortices is greatly enhanced for small  $\theta_{01}$  and leads to the appearance of secondary streamwise vortices which are stretched between consecutive vortices of the inner and of the outer shear layer. The transition towards a fully developed turbulent state is strongly linked with the formation and stretching of these streamwise vortices. The critical value  $\lambda_c$ , separating the regime without and with recirculation bubble is found to be strongly dependent on  $\theta_{01}$ .

For  $\lambda > \lambda_c$ , the shape and the length of the recirculation bubble is seen to be strongly affected by the shape of the inlet profile: the bubble is indeed significantly shortened when  $\theta_{01}$  is small. The downstream region of the bubble is the siege of intense longitudinal vorticity production yielding the generation of intense streamwise vortices. Again these vortices are associated with a fast flow three dimensionalization and rapid transition to turbulence.

The thickness of the inner shear layer also affects the evolution of the global quantities such as the jet spreading rate and the length of its two potential cores. For large enough values of  $\lambda$ , the entrainment by the outer jet leads to an important depletion of the fluid situated near the jet axis. This depletion is associated with a low-pressure region in the jet core and with a curvature of the main velocity streamlines towards the jet axis: this creates a diminution of the jet width corresponding to a pinching phenomenon. This pinching phenomenon is more and more pronounced when  $\theta_{01}$  decreases.

The initial pinching stage is followed by a stage of linear spreading characteristic of a turbulent regime. The linear growth is reached at shorter downstream distances when  $\theta_{01}$  is small due to the faster turbulence growth within the jet core. The pinching phenomenon is seen to reach a saturation level for  $\lambda > \lambda_c$ .

In numerical studies of the effect on the level of initial turbulence on the mixing made by Barata et al. [39 & 40], the rate of mixing is larger when the outer jet has more velocity than the inner jet and it is dependent of the velocity ratio. With the change of the turbulence intensity of the outer jet, it appeared that the zone of recirculation switch back on the position until the disappearance on the maximum limit. The location of the center of the recirculation zone is almost constant. In the case of reasons diameter close to 1, the variation in levels of turbulence intensities of the jet have much influence.

Ribeiro and Whitelaw [41] made their measurements in a coaxial jet flow of a mean velocity ratio of unity. They focused their attention to the region of flow in the wake of the wall of the inner pipe to assess its influence on the mixing and on assumptions which are frequently made in turbulence modeling. They concluded that for equal maximum initial velocities, i.e. mean-velocity ratio of unity; a coaxial jet develops faster than a single jet and the conditions for self-preserving were almost satisfied for the mean velocity radial profiles at seventeen outer diameters but the radial profiles of the Reynolds shear stress did not confirm with the self-preserving pattern at this location.

### *1.3 Motivation*

The turbulent mixing of coaxial confined jets is a complex dynamic process that is applied in a large number of devices such as the engineering ejectors, pumps jet, industrial burners, combustion chambers of jet engines, nuclear rockets gas, mixing chambers of turbofans, afterburners, and so on. The study of the aerodynamic performance of coaxial jets in different types of confinement also has a fundamental interest because it involves the interaction of different turbulent flow phenomena, whose details are not yet very well known quantitatively. The parameters that are involved in the process of mixing and are primarily responsible for the complexity of the process are both geometric or operational parameters such as: velocity, temperature or density ratios, compressibility effects, levels of turbulence of jets, pressure gradient, interaction between the walls and the jets or the ration between the diameters of the mixing duct and the internal jet nozzle.

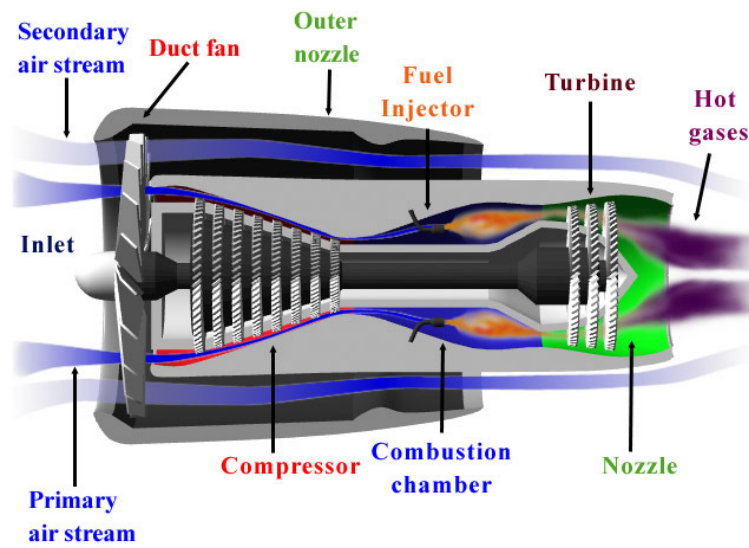


Fig. 3 Schema of a turbofan engine

With optimal conditions for the parameters involved, the possibility of having more efficient engines, cheaper, less noise and less polluting will become certitude. It is necessary to study all these parameters and to find an optimal interaction with all these parameters.

The aim of the present work is to study the effect of  $\theta$  on the flow development and to identify the associated regimes, and in particular the production of a flow reversal in the central zone near the jets exit.

## CHAPTER 2

### *2 Experimental Method*

#### *2.1 Introduction*

This chapter presents the Experimental Setup and the method used to measure the flow velocities in this experimental study by using Laser Doppler Anemometry or LDA. This Chapter concerns the design of the Wind Tunnel and the explanation of the LDA technology and all the necessary devices.

#### *2.2 Description of the Wind Tunnel Design.*

To study the mixing of Confined Coaxial Jets, the Experimental Setup was designed according with the available experimental conditions. Considering the complexity to design and build a Wind Tunnel able to simulate a Coaxial Jet, it has been decided that the simulation should be a two dimensional planar flow show on Figure 4.

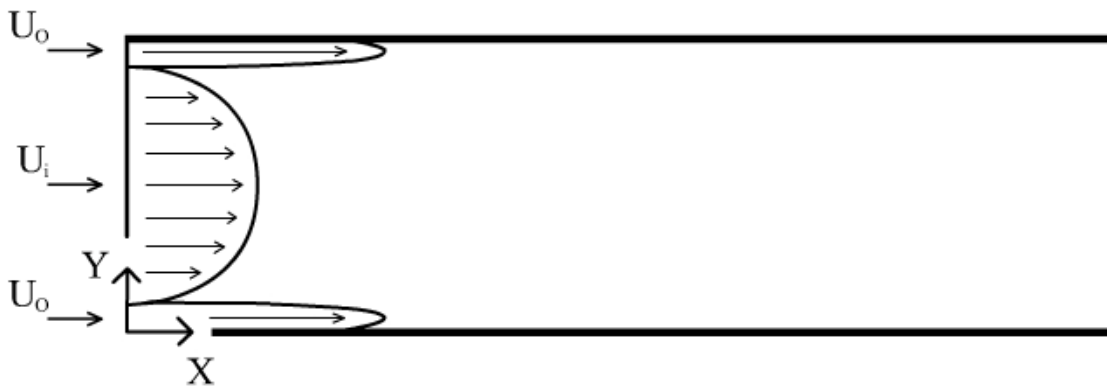


**Fig. 4 Experimental Method**

A bi-dimensional configuration was adopted as shown schematically in Figure 4. All the test section was confined by an upper and under wall and the input flow was done by an inner flow  $U_i$  and an outer flow  $U_o$  with different velocities.



The Wind tunnel use for the present work was the same used by Barata et al.(2005) [44], but with a change on the output flow. The design and the implementation of this change on the Wind Tunnel were done according to Metha R.D. and Bradshaw P. (1979).[42,43].

The Wind Tunnel used by Barata et al.(2005) [44] is an open Wind Tunnel. It uses a centrifugal Blower with a capacity of 3000m<sup>3</sup>/h at 2935 rpm and with a nominal power of 15kW. The dimensions at the test section are 300mm height and 280mm width.

The change designed for the Wind Tunnel was considering this data and according Metha R.D. and Bradshaw P. (1979) [42,43]. The principal equation for the design was the Continuity Equation, the rate at which mass enters a system is equal to the rate at which mass leaves the system.

$$\frac{\partial \rho}{\partial t} + \nabla \cdot (\rho u) = 0 \quad (1)$$

For incompressible flow,  $\nabla \cdot u = 0$  (2)

In a simple way,  $\rho_1 u_1 A_1 = \rho_2 u_2 A_2$        $\rho_1 = \rho_2$  (3)

$$u_1 A_1 = u_2 A_2 \quad (4)$$

The goal of the Wind Tunnel was to produce a velocity ratio about 1.5, 3, 6 and 10 to compare with numerical simulation done by Barata et al [38, 39]. So, four different Wind Tunnel adaptations were designed, but only the adaption for  $\lambda=6$  was tested. The convergent divergent angle used in the Wind Tunnel adaption was 7° (Metha R.D. and Bradshaw P. (1979)). Until 7,5°, there is no possibility of separation of the flow from the walls. At the exit, the separating plates of the inner jet and the outer jet were extended 0.2 D horizontally, to eliminate the vertical component of the velocity produced by the divergent/convergent (Metha R.D. and Bradshaw P. (1979)). The Dimensions of the four Wind Tunnel Adaption's are presented on the following table.

$\lambda$	1,5	3	6	10
h1 [m]	0,027	0,046	0,071	0,090
h2 [m]	0,245	0,207	0,079	0,060
h1' [m]	0,020	0,020	0,020	0,020
h2' [m]	0,260	0,260	0,260	0,260
L [m]	0,065	0,219	0,419	0,573
0,2Dhid [m]	0,068	0,068	0,068	0,068
Ltotal [m]	0,133	0,287	0,486	0,641

Table 1 Dimensions of the Wind Tunnel Adaption for  $\lambda=1.5, 3, 6$  and  $10$ .

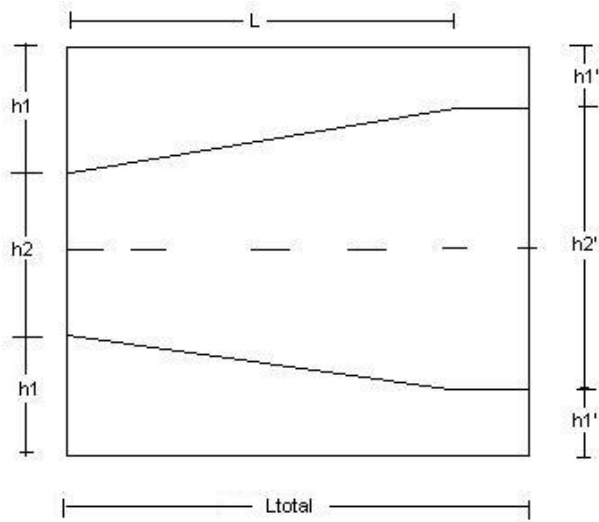


Fig. 5 Schema of the Designed Wind Tunnel

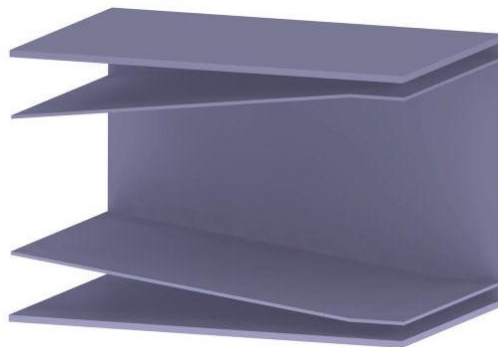
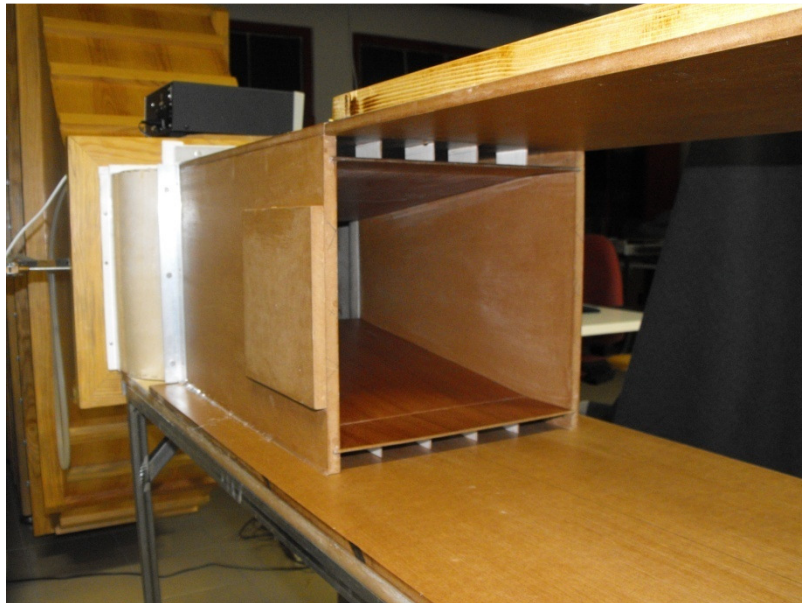


Fig. 6 Draw of the Designed Wind Tunnel for  $\lambda=6$ .

The flow inside the Wind Tunnel was accelerated by the convergent producing the outer jet and the inner jet was slowed by the divergent. The test section had 1 meter long and the flow was confined superiorly and inferiorly by two slabs of wood simulating the walls of a turbofan engine. To create turbulence on the outer jets and to create a bigger turbulence intensity ratio, 4 plates were introduced vertically and evenly spaced near to the exit of the outer jets.



**Fig. 7 Picture of part of the Wind Tunnel with details of the convergent and divergent**

During the first tests on the Wind Tunnel, it was verified that the velocity ratio of 6 was not achieved. The air has the ability to adapt itself to the obstacles and splitter plates on the adaption. So, the flow simply flows through the areas where it was easier to pass. This was verified during the flow visualization. Most of the flow was directed to the divergent (inner jet). The pressure inside the wind tunnel was quite equal on the exit, that's why the flow was capable to adapt itself to the Wind tunnel.

To solve this situation, it should be built a completely new wind tunnel to simulate Coaxial jets. There was no time for that, a sandwich honeycomb with a grid was introduced at the entrance of the convergent and the velocity ratio was increased for a value of  $\lambda=2$ . An incidental effect of honeycombs was to reduce the turbulence level in

the flow. Essentially, the lateral components of turbulence, like those of mean velocity, are inhibited by the honeycomb cells. Honeycombs themselves shed small scale turbulence. With this honeycombs, the ratio of turbulence intensities was increased between the two jets. The grid causes a pressure drop decreasing the inner velocity and increasing the outer velocity.

The Wind Tunnel adaption, the confinement and the test section were built in the DCA Aerospace Sciences Department of the University of Beira Interior. The materials used on this building were mainly wood (MDF) due to the ease of working the wood and the low price of purchasing.



**Fig. 8 Wind Tunnel and Test Section**

The construction process consisted mainly in cutting and assembling the various pieces which form the tunnel after the drawings were printed in actual size. This work was done by Mr. Rui Paulo from the Aerospace Sciences Department.

## 2.3 Description of the method

### 2.3.1 Principles of LDA

The acquisition of data has been done using a LDA *Dantec FlowLite 2D* system. Laser Anemometers are non-intrusive instruments for the investigation of fluid flow structures in gases and liquids. Laser anemometers probe the flow with focused laser beams and can sense the velocity without disturbing the flow in the measuring volume. The only necessary conditions are a transparent medium with a suitable concentration of tracer particles or seeding and optical access to the flow through submerged optical probe. The LDA technology doesn't measure the velocity of the flow itself, but the velocity of the particles suspended on the flow. The measurement is based on the stability and linearity of optical electromagnetic waves, which for most practical purposes can be considered unaffected by other physical parameters such as temperature and pressure. The quantity measured by the laser Doppler method is the projection of the velocity vector on the measuring direction defined by the optical system. The optics of the laser anemometer is able to define a very small measuring volume and thus provides good spatial resolution and allows local measurement of Eulerian velocity. The small measuring volume in combination with fast signal processing electronics also permits high bandwidth, time-resolved measurements of fluctuating velocities, providing excellent temporal resolution. The temporal resolution is limited by the concentration of seeding rather than the measuring equipment itself.

Laser Doppler Anemometry is based on Doppler shift of the light reflected from a moving seeding particle.

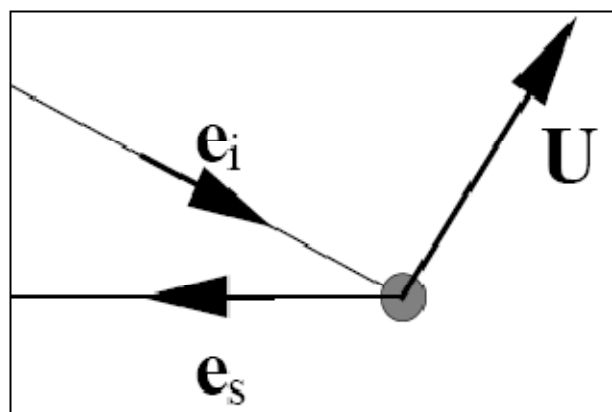


Fig. 9 Light Scatter from a moving seeding particle

The main idea is shown on Figure 9 , where the vector  $U$  represent the particle velocity, and the unit vectors  $e_i$  and  $e_s$  describe the direction of incoming and scattered light respectively. The light is scattered in all directions at once, but we consider only the light reflected in the direction of the receiver. From the receivers' point of view, the seeding particle act as a moving transmitter and the movement introduce additional Doppler-shift in the frequency of the light reaching the receiver. For two intersecting laser beams, the light is scattered as illustrated on the following figure:

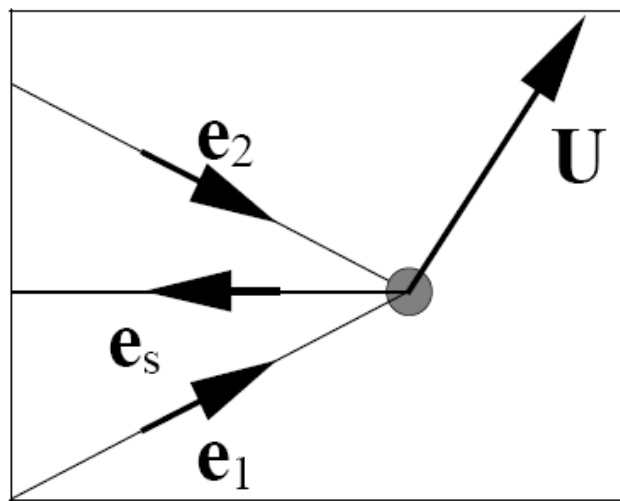
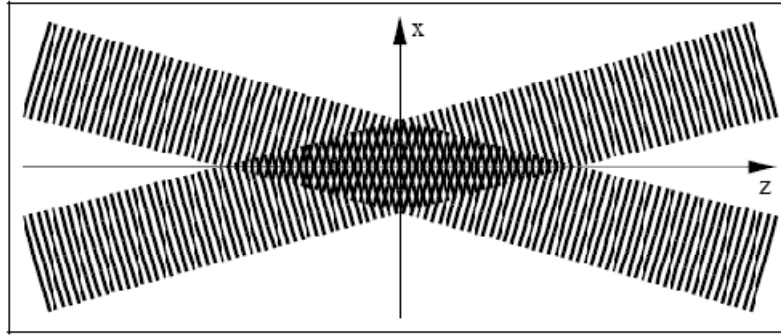


Fig. 10 Scattering of two incoming laser beams

Both incoming laser beams are scattered towards the receiver, but with slightly different frequencies due to the different angles of the two laser beams.

The fringe model is commonly used in LDA as a reasonably simple visualization producing the correct results. If the beams intersect in their respective beam waists, the wave fronts are approximately plane, and consequently the interference produce parallel planes of light and darkness as shown in figure 11.



**Fig. 11 Fringes form where two coherent laser beams cross**

The interference planes are known as fringes. The fringes are oriented normal to the  $x$ -axis, the intensity of light reflected from a particle moving through the measuring volume will vary with a frequency proportional to the  $x$ -component  $u_x$  of the particle velocity.

Measurements take place in the intersection between the two incident laser beams. Due to the Gaussian intensity distribution in the beams, the measuring volume is an ellipsoid. The LDA used is a Backscattered LDA.

The primary result of a laser anemometer measurement is a current pulse from the photodetector. This current contains the frequency information related to the velocity to be measured.

The photomultiplier converts the light intensity to electrical fluctuations signals which are in turn converted to velocity information in the BSA processor. The frequency of the flashing light (Doppler frequency) is proportional to the flow velocity at the measurement point. The processing results are handled by the BSA Flow Software. Three components of the velocity vector can be acquired simultaneously, depending on the system configuration.

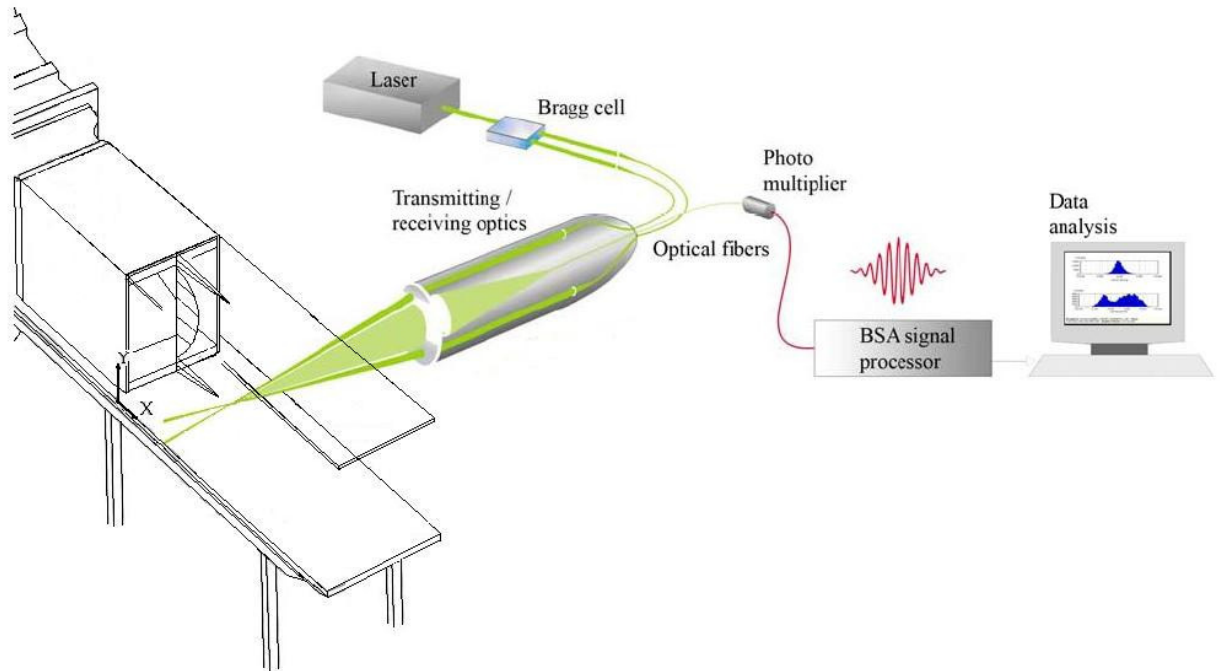


**Fig. 12 Diagram of the Experimental Setup with Laser**

This LDA Flowlite 2D uses a dual beam configuration with a backscattered optical system. This system uses a He-Ne laser with an output of 10mW and a laser diode of 25mW. The sensitivity to the direction of flow was introduced by a frequency  $f_0 = 40\text{MHz}$  generated in a Bragg cell. It has been used a lens with a focal length of 400 mm in the light emitter. The value of half angle formed between rays is  $2.8^\circ$  and the size of the volume control (ellipsoid form) is:  $135 \times 6.54 \times 6.53 \mu\text{m}$  and  $112 \times 5.46 \times 5.45 \mu\text{m}$ , using the size definition of the radius based on intensity  $e^{-2}$ . The horizontal component  $U_{\text{mean}}$  and vertical component  $V_{\text{mean}}$ , and the fluctuations were calculated by the processor Dantec BSA F60. This processor has the characteristic that has two channels prepared to calculate the velocities.



Wave Length, $\lambda$ [nm]	633 (He-Ne)	532 (Diode Laser)
Focal Length between Lenses, $f$ [mm]	400	400
Beam Length, defined by the intensity $e^{-2}$ [mm]	1.35	1.35
Spacing between beams, $s$ [mm]	38.87	39.13
Half Angle of Beam Intersection, $\theta$ [°]	2.78	2.8
Spacing between fringes, $\partial f$ [ $\eta\text{m}$ ]	6.53	5.45
Transfer Constant of the Speedometer, $K$ [ $\text{MHz}/\text{ms}^{-1}$ ]	0.153	0.183

**Table 2 Characteristics of Dantec LDV Flowlite 2D**

The transmitting/receiving optics system has been placed in a tridimensional traverse (directions X, Y, Z). The traverse is directly controlled by BSA Flow Software and the Control Volume can be moved for a minimum of 0,1mm.



**Fig. 13 Traverse System with the transmitting/receiving Optics System**

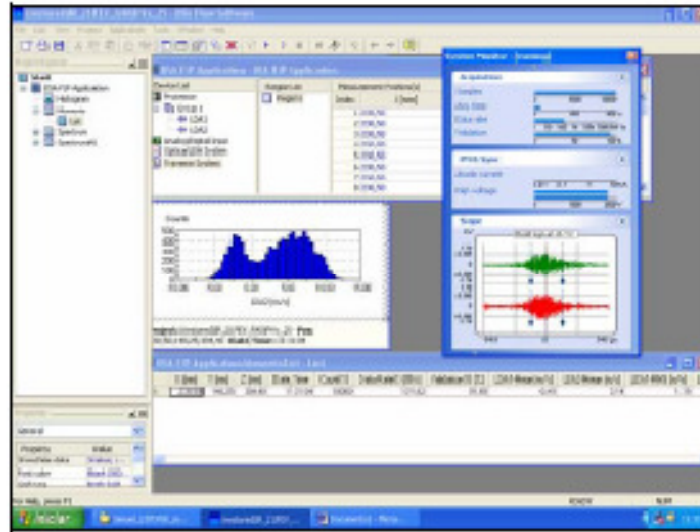


Fig. 14 Software BSA FLOW

### 2.3.2 Seeding

In Laser Doppler Anemometry, it is not the velocity of the flow that is measured, but the velocity of particles suspended in the flow. The seeding is considered the actual velocity probes. The particles must be small enough to track the flow accurately, but large enough to efficiently scatter sufficient light for the photodetector to be able to detect the Doppler frequency.

The choice of seeding depends on a number of parameters. The particles need to be able to follow the flow and good light scatterers, but the shape of the particles affect the drag exerted on the particle by the surrounding fluid. The particle concentration affects particle motion through interaction between different particles. So, it is necessary to use low concentrations of seeding. For normal and fast flows, the body forces, such as gravity, can be neglected.

In this Experimental Setup, the seeding has been made by a smoke machine *Techno-Fog Jem*. This seeding was accumulated in a reservoir at a pressure value of 1.5 bar and then send into the Wind Tunnel. The typical diameter of the seeding particles in the air flow is between 0,1 and 1  $\mu\text{m}$ . The smoke was injected inside the tunnel at a pressure of 2 bar. The data rate during the experience remained at 130Hz and a data validation bigger than 90%.



Fig. 15 Seeding machine

#### *2.4 Alignment and Calibration of the Experimental Setup*

The alignment and the calibration of the experimental setup was done to have always the same conditions for the experience and to minimize the errors on the equipment during the measurements.

The table of the test section was fixed and aligned to the Wind Tunnel and parallelly to the bars fixed on the ground of the Traverse System. The Wind Tunnel adaption (Coaxial jets) was subsequently added to Wind Tunnel and fixed to the exit. Through the Laser Doppler Velocimetry, a laser beam was projected to the wall of the Wind Tunnel adaption and moved parallel to the experimental Setup. When the intensity of the laser beam on the wall was constant by moving parallelly, the Wind tunnel adaption was considered aligned and fixed at the main Wind Tunnel on this position.

The parallel bars fixed on the ground were added to enable the Traverse System to analyze all the test section with the laser beam. The Seeding was introduced on the Wind Tunnel by thin tubes on the center of the Wind Tunnel that were connected to the smoke machine. The volume control was situated at the middle of the test section parallel to the table and Wind Tunnel.

### *2.5 Measurements*

The data was obtained with the measurement of 9 vertical profiles over X. The frequency of the blower was close to 41 Hz. It was used a digital multi-gauge Furnance FCO 12, capable of measurements between 1 and 20 mmH<sub>2</sub>O. This multi-gauge presents a maximum error of  $\pm 1\%$ . The value of dynamic pressure of 1.15 mmH<sub>2</sub>O was controlled to maintain the conditions for measurements in experimental section. This value of pressure was also a reference to the repeatability of measurements, since the calculation of the pressure dynamics in multi-gauge don't use the temperature. This also helped to keep the flow characteristics of the flow for each measurement performed.

To increase the precision of the data obtained on the measurements, 10000 samples of seeding were measured for each point on the vertical profile to obtain the velocities and the fluctuations. The Statistical errors are less than 1.5 and 3% respectively, for the average value and variance, according with the analysis of Yanta et al. (1973).

## CHAPTER 3

### *3 Results*

#### *3.1 Introduction*

The Experimental Results will be discussed on the following chapter. This chapter includes four sub-chapters. Firstly, the discussion of a qualitative visualization of the 2D coaxial flow recorded by a cam recorder will be presented. Secondly, the vertical profiles of mean velocities and fluctuating velocities obtained by LDV will be discussed. Thirdly, the mean velocities field characteristics and his Isolines will be analyzed and finally, the shear layer characteristics will be presented and discussed.

#### *3.2 Visualization*

With the operational Wind Tunnel, the first experimental work was to visualize the flow and the mixing of the two layers on the confined test section. But firstly, some initial measurements were performed with the Pitot tube to check the uniformity of flow coming out of the co-axial ducts. The profiles showed that the flow is quite uniform and. the velocities of the inner and outer jet were measured. The conditions of the blower of the Wind tunnel and the pressure variation were the following:

$$f = 41,2\text{Hz}$$

$$\Delta p = 1,15\text{mmH}_2\text{O}$$

The inner jet presented a value of 8m/s and the outer jet 15,4m/s.

$$U_i = 8\text{ m/s}$$

$$U_o = 15,4\text{ m/s}$$

$$\lambda = \frac{U_o}{U_i} \cong 2 \quad (5)$$

(6)

The velocity ratio was determined by the outer and inner jet velocities. The ratio velocity was equal to 2.

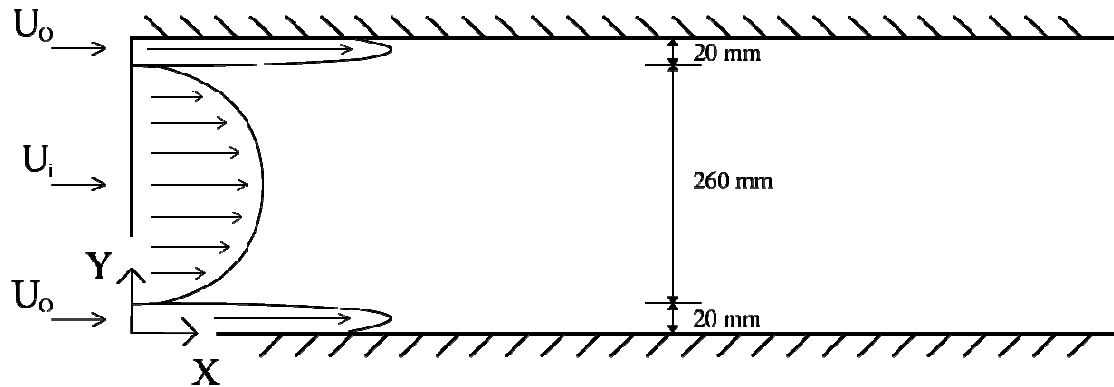


Fig. 16 Schema of the Experimental Setup

To visualize the flow, seeding in large quantities and in a constant flow has been introduced on the outer jets inside the Wind Tunnel aligned with the volume control. More detailed visualization studies were performed with a digital camera (SONY DCR-VX2100 PAL). The camera shutter speed was set to 25 frames/second to the best compromise between image contrast and time integration of tracer particle velocities. The visualization movie was separated frame by frame with the Adobe Premiere Software.

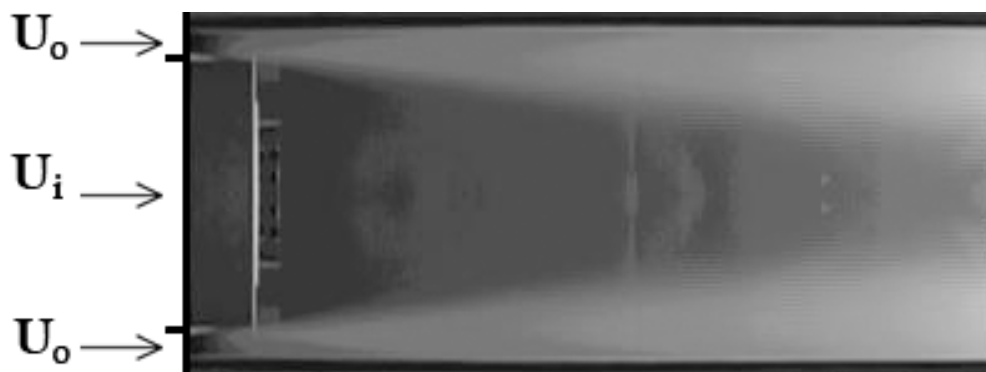


Fig. 17 Mean Flow Concentration for  $\lambda=2$

This image was obtained after image processing by MATLAB. The frames obtained by Adobe Premier Software were treated and transformed in grey-scale images. After this, with some images, a mean flow concentration image corresponding to the flow was created.

On the Figure 17, the exit of the wind tunnel is on the left and the flow is developing to the right. The test section is 300 mm high and 800mm long on the image. At the exit of the wind tunnel, there is the initial merging zone wherein the inner and the outer streams enter the mixing test section with different uniform axial velocities as shown on figure 15. On this initial zone, the flow consists of two different potential flow regions as Ahmed & Sharma [1] explained. As it can be seen, the outer jet (with bigger velocity) spreads towards the center mixing itself with the inner jet. Acharya[3] verified that the turbulent friction between the two streams is larger in confined jets than in unconfined jets and that the absolute value of the difference of velocities between the two streams considerably influenced the mixing between the two jets by enhancing the momentum transfer between them. There is a continuous exchange of momentum between the inner and outer streams. Further downstream on the right of the picture, the flow conditions become progressively similar of those of a single jet [2, 3] and the inner potential core disappeared.

### *3.3 Vertical Profiles:*

The achievement of the measurements was done by LDV and 9 vertical profiles were measured along 250mm from the output of the jets. The first vertical profile was measured in the complete vertical length of the test section ( $Y=300\text{mm}$ ) at  $X/b=0,9$ . The first vertical profile was measured at a small distance of the exit, because of the difficulty in focusing the laser beams at those locations. The results are demonstrated on the following graph.

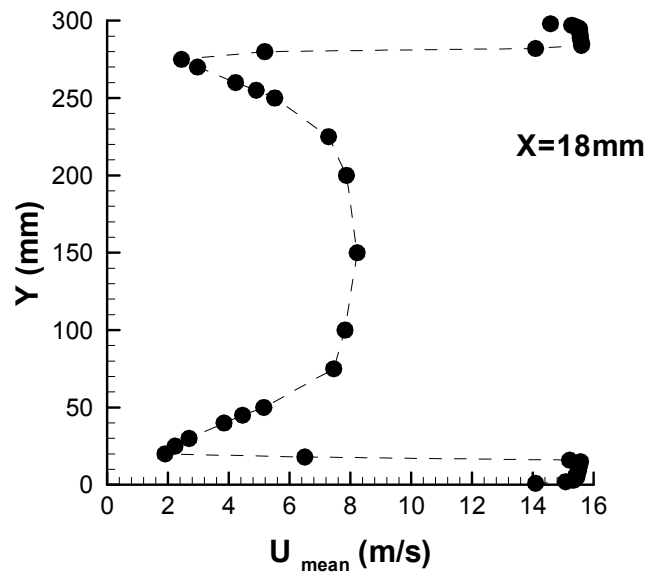


Fig. 18 Complete Vertical Profile of  $U_{\text{mean}}$  for the first station

Care was taken to ensure the flow axisymmetry. The Graphic shows that the minimum velocity  $U_{\text{mean}}=2$  m/s is obtained for  $Y=20$ mm and  $Y=280$ mm, it is the zone were the inner jet is separated from the outer jet by a splitter plate on the wind tunnel. For the inner jet, the maximum value  $U_{\text{mean}}$  is about 8 m/s at the middle of the height of the test section  $Y=150$ mm. For the outer jets, the velocity profile is similar for the two outer jets and rising  $U_{\text{mean}}=15.4$  m/s. The results of the mean horizontal velocities  $U_{\text{mean}}$  for  $X=18$ mm ( $X/b=0.9$ ) shows that the flow is symmetric for the axis  $Y=150$ mm.

The measurements for the 9 vertical profiles were done just for half of the height of the test section since it was established the symmetry of the flow.

The results of the mean velocities are showed on Figure 18. The graphs were dimensionally using the value  $b$  as the height of the exit of the outer jet,  $b=20$ mm.  $U_{\text{med}}$  was calculated using the following equation:

$$U_{\text{med}} = \frac{U_i \cdot A_i + U_o \cdot A_o}{A_i + A_o} = 9 \text{ m/s} \quad (7)$$



Analyzing the Figure 19, for  $X/b=0.9$  for  $U/U_{med}$ , it was easily observed the difference between the inner jet and the outer jet. The outer jet presented a vertical profile well defined in order of  $U/U_{med} = 1.7$  for  $0 < Y/b < 1$ . On the separation of the outer jet and inner jet  $Y/b=1$  by the splitter plate, it is observed a peak in that the horizontal mean velocity is about  $U/U_{med} = 0.2$  and the inner jet profile starts from this value evolving to  $U/U_{med} = 0.9$  at  $Y/b=7.5$ .

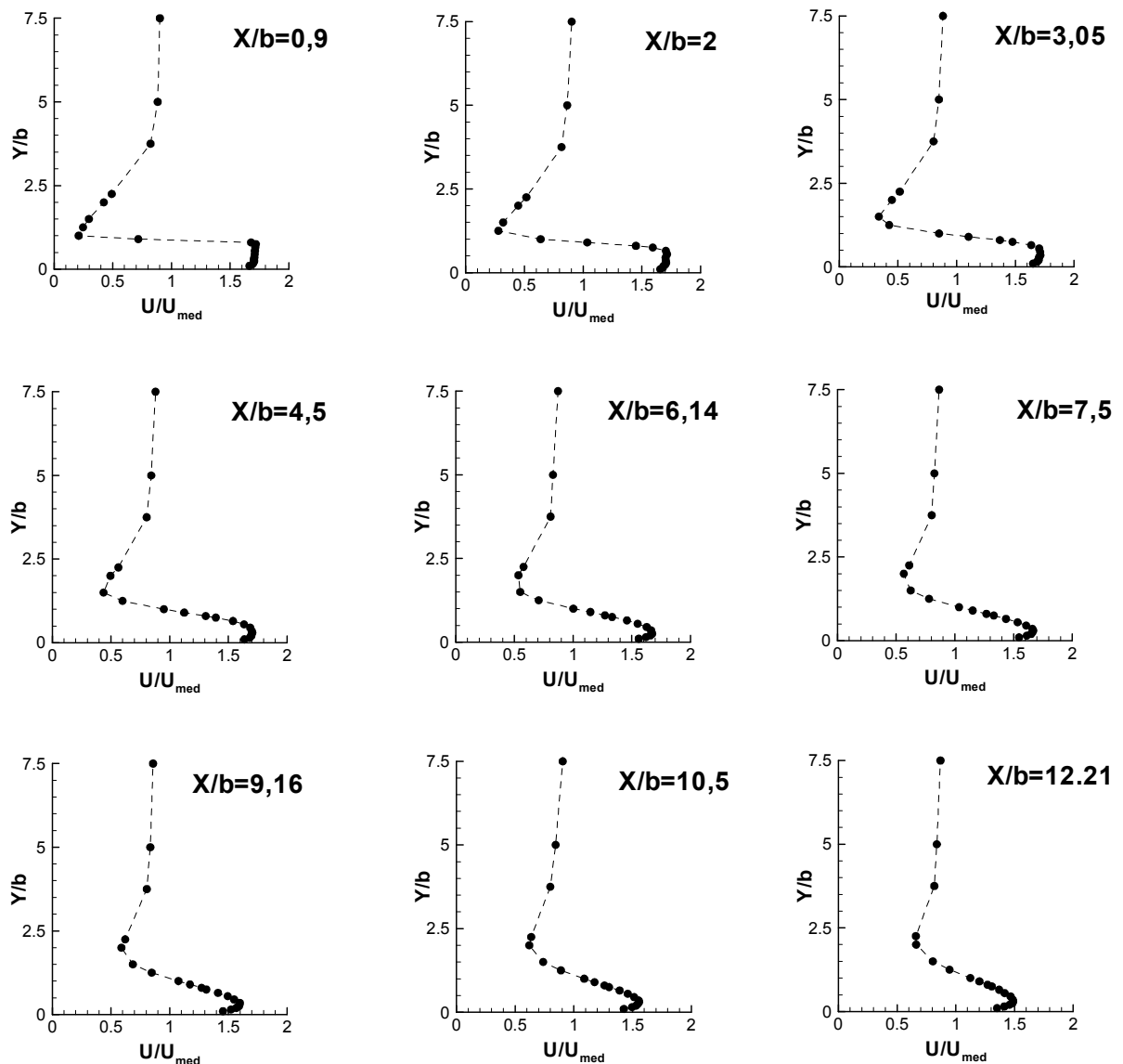


Fig. 19 Vertical Profiles of Mean Velocities Characteristics  $U/U_{med}$

Observing the following positions  $X/b=2$ ,  $X/b=3.05$  and  $X/b=4.5$ , the peak at  $Y/b=1$  started too soft while the  $U/U_{med}$  was accelerated by the outer jet. However, the velocity of the outer jet was decreasing while the inner jet velocity profile increased his velocity between  $1 < Y/b < 3$ . For  $3 < Y/b < 7.5$ , the outer jet profile maintained the same values. From  $X/b=6.14$ , the well defined peak of the minimum  $U/U_{med}$  for  $Y/b=1$  disappears while the horizontal velocity is increased.

Along  $X/b=7.5$ ,  $X/b=9.16$ ,  $X/b=10.5$  and  $X/b=12.21$ , the outer jet decreased his mean horizontal velocity to values of  $U/U_{med} = 1.5$  for  $Y/b=0.5$  and the inner jet accelerated between  $1 < Y/b < 3$  to equal the horizontal mean velocity to 0.9 find in  $3 < Y/b < 7.5$ . This is due to entrainment.

It is to preview that the outer jet horizontal mean velocity will decrease until equal the inner jet horizontal mean velocity while the inner jet will accelerate between  $1.5 < Y/b < 3$ . For a farther zone, the vertical profile will have the same form as a single jet.

For the Figure 20,  $V/U_{med}$ , for  $X/b=0.9$ , the mean vertical velocity component is always positive, except on the region were the inner jet is separated by the splitter plate of the outer jet  $Y/b=1$ . The values of the mean vertical velocities are quite small. The maximum value of the mean vertical velocity is find for  $Y/b=2.3$ . At the exit, mainly in the outer jet, the flow is quite horizontal, without big vertical velocities. Between  $1.5 < Y/b < 7.5$ , the mean positive vertical velocities decrease as long as the flow progresses. The major differences are on  $0 < Y/b < 1.5$ .

At the level of  $1 < Y/b < 1.5$  for  $X/b=2$ ,  $X/b=3.05$  and  $X/b=4.5$ , the flow converge to negative mean vertical velocities. At  $X/b=2$ , there is a peak on the negative velocity for  $Y/b=2$ , and it also presents the biggest difference between velocities.

For  $X/b=6.14$  until  $X/b=12.2$ , between  $0 < Y/b < 1.5$ , the flow pass to negative vertical values, but really close to 0. The tendency is to reach the vertical velocity 0.

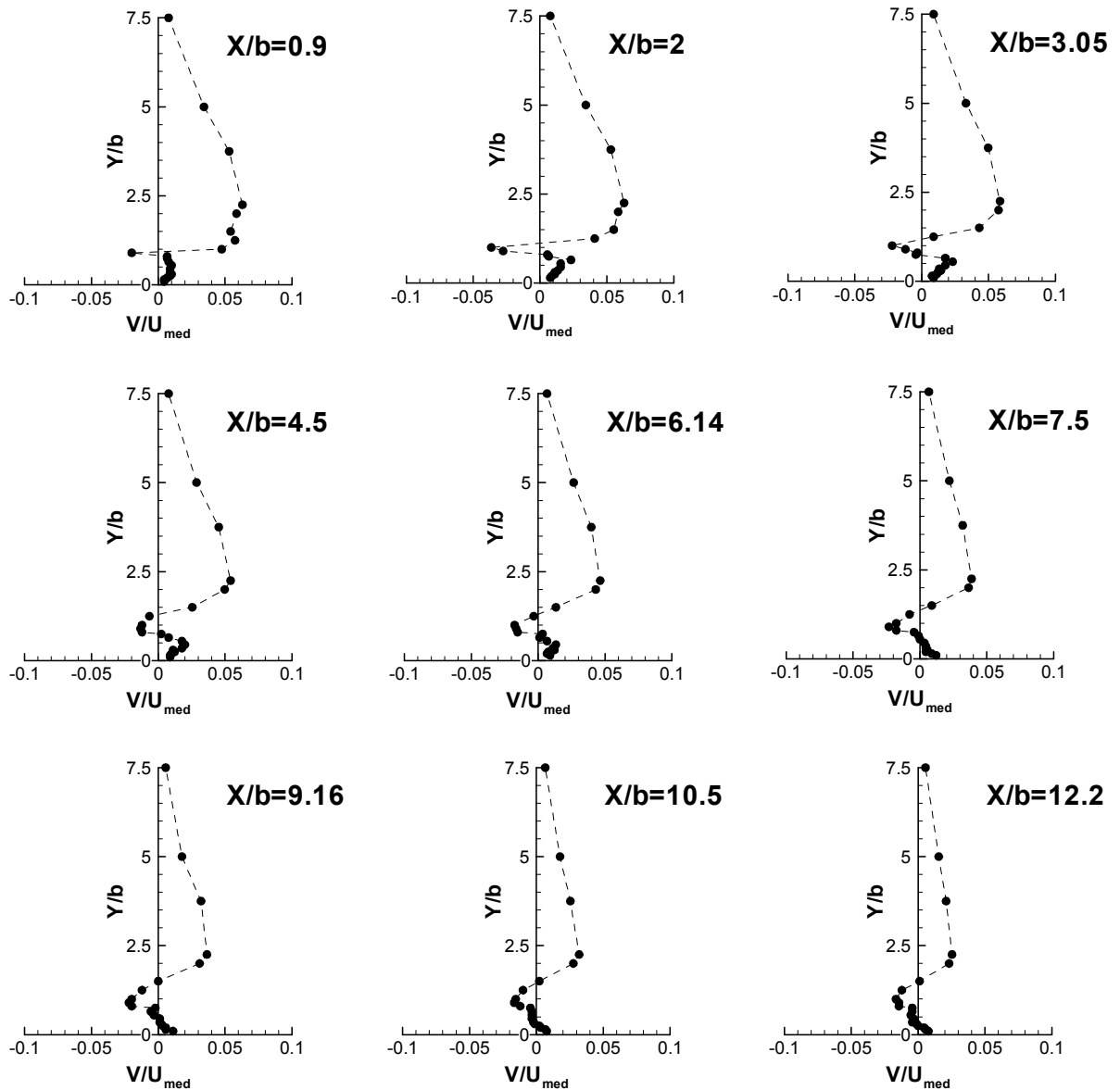


Fig. 20 Vertical Profiles of mean velocities characteristics  $V/U_{med}$

Figure 21 and 22 shows the turbulent velocity characteristics for horizontal and vertical velocities. For the horizontal turbulent velocity, it can be seen that the turbulence intensity varies on values around 0.28, except for  $1 < Y/b < 2$ , where it is located a peak of turbulence intensity about 0.35. This is probably due to the splitter plate between the inner jet and the outer jet. As long as the flow progresses, the peak of turbulence intensity for  $Y/b=1$  increase to  $u'_{RMS}/U_{med}=0.44$ . After  $X/b=2$ , the turbulence intensities starts to decrease in generally except for  $0 < Y/b < 1$ , where the turbulence intensity

increase due to the vertical plates introduced on the outer jet causing turbulence. That's why the inner jet is quite uniform in his turbulence for  $Y/b > 2$ .

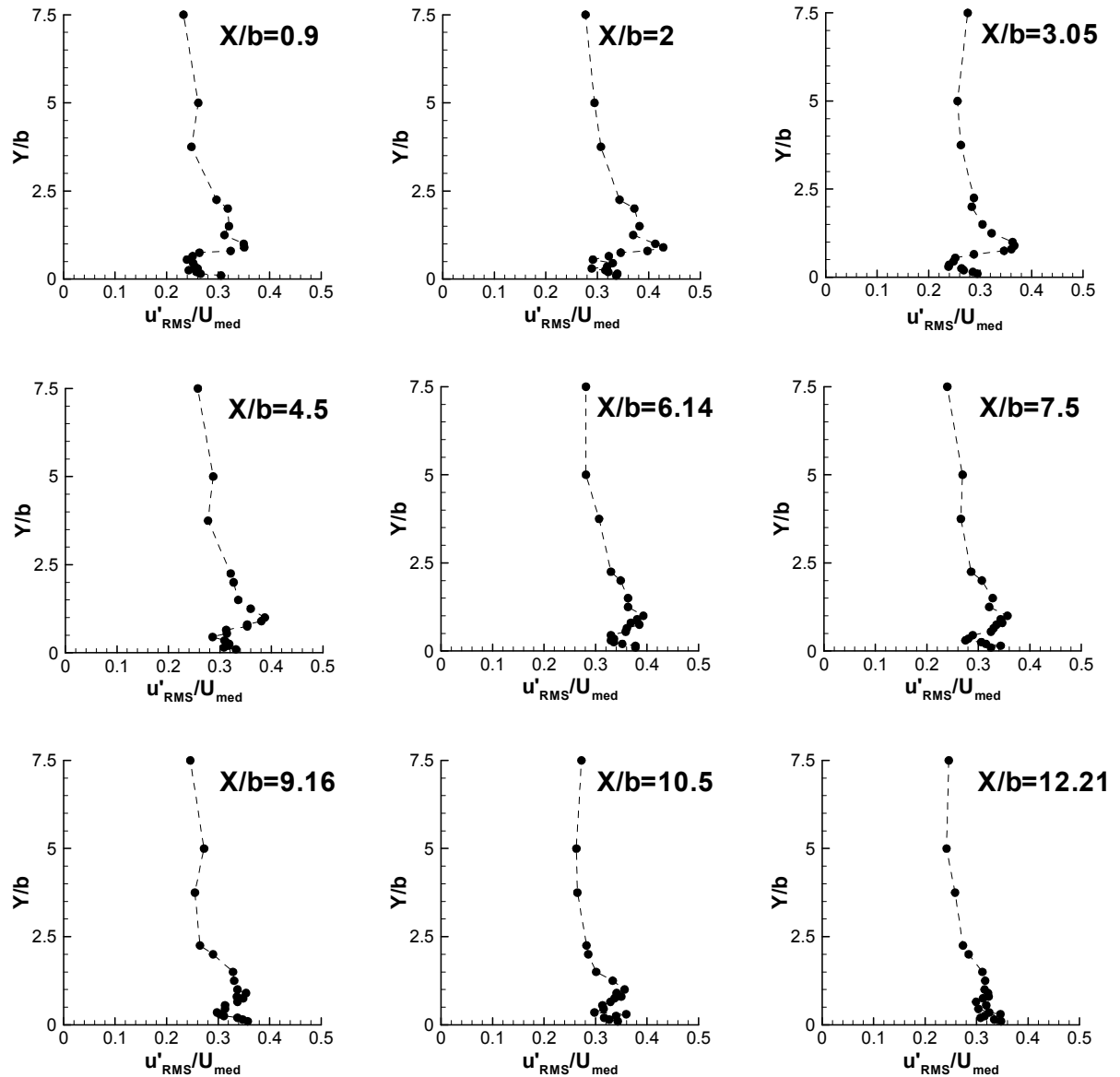


Fig. 21 Vertical Profiles of fluctuating velocities  $u'_{RMS}/U_{med}$

For the vertical turbulent velocity at  $X/b=0.9$ , the turbulence intensity is quite uniform, except for  $Y/b=1$ , where it is located a peak of turbulence intensity about 0.34. This is due to the splitter plate between the inner jet and the outer jet. As long as the flow progresses, the peak of turbulence intensity for  $Y/b=1$  decrease, but in generally for  $0 < Y/b < 2$  the fluctuations increase until  $X/b=12.21$ . This increase is also due to the

vertical plates introduced on the outer jet causing turbulence. That's why the inner jet is quite uniform in his turbulence for  $Y/b > 2$ .

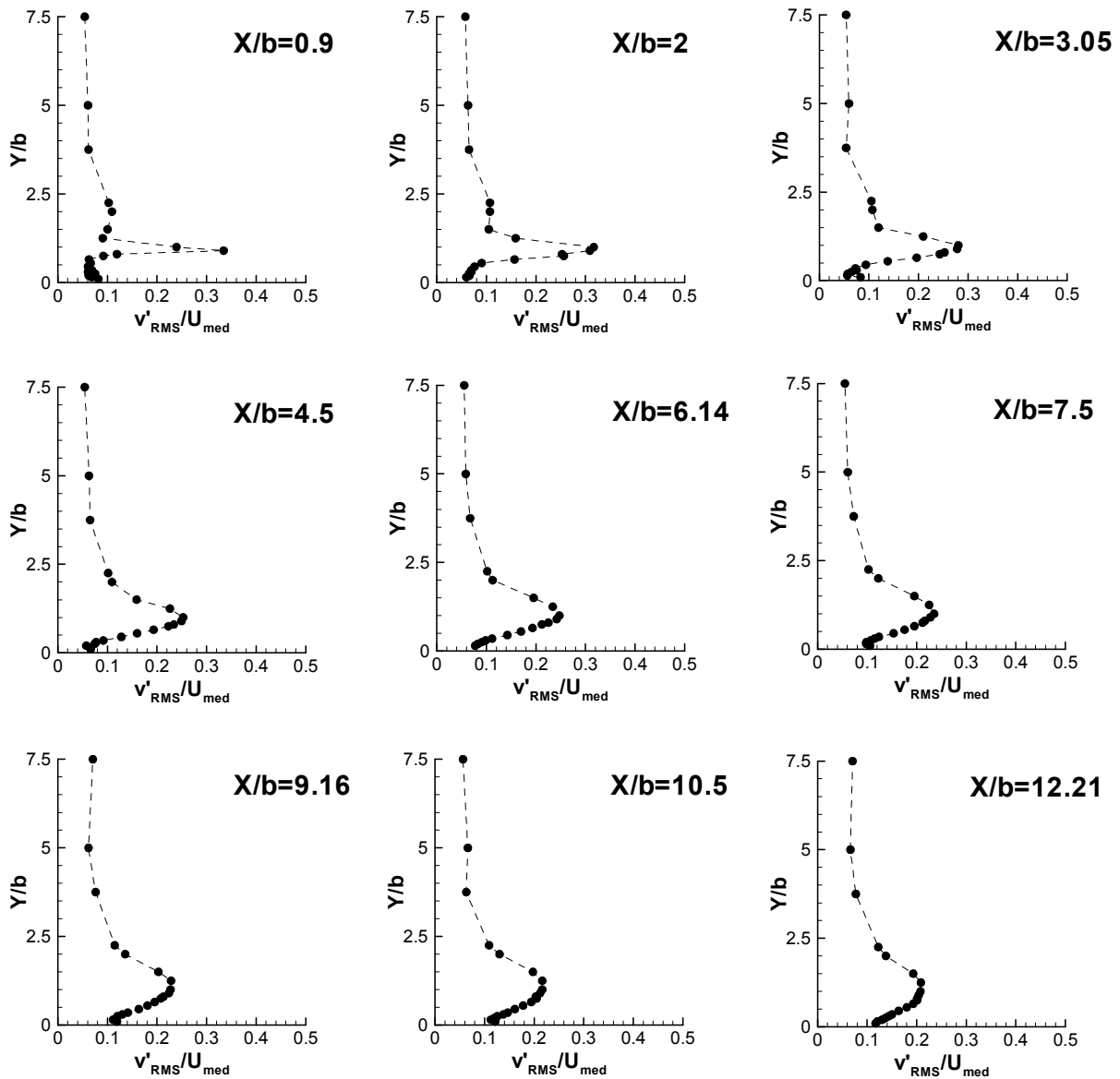


Fig. 22 Vertical Profiles of fluctuating velocities  $v'_{RMS}/U_{med}$

The peaks of  $\sqrt{v'^2}$  are larger than the corresponding peaks and of  $\sqrt{u'^2}$  and the curves on the graphics for  $\sqrt{v'^2}$  are smoother.

Through the vertical profiles, the ratio of turbulence intensity is determined by the following equations:

$$\theta = \frac{\frac{\sqrt{u'^2_o}}{U_{med}}}{\frac{\sqrt{u'^2_i}}{U_{med}}} = \frac{\sqrt{u'^2_i}}{\sqrt{u'^2_o}} \cong 1.5 \quad (8)$$

$\sqrt{u'^2_i}$  = value of the fluctuation of the  $U_{mean}$  velocity for the inner jet

$\sqrt{u'^2_o}$  = value of the fluctuation of the  $U_{mean}$  velocity for the outer jet

The ratio of turbulence intensity is about 1.5 at the exit of the Wind Tunnel on the region of interaction of the inner jet and outer jet. Higher turbulence level favors faster mixing on a two streams flow [13, 14].

### 3.4 FlowField

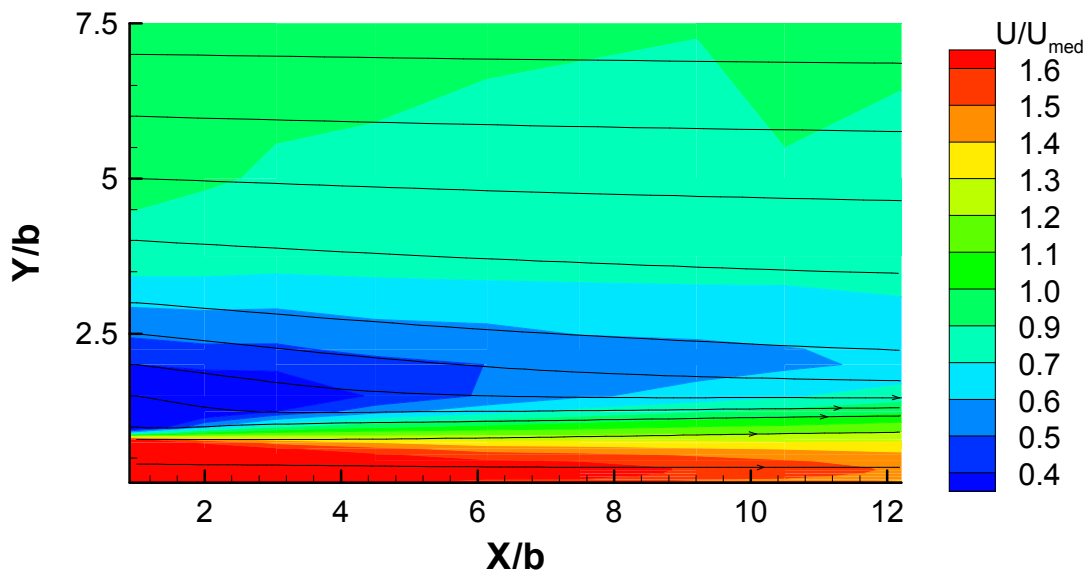


Fig. 23 Isolines of mean velocity characteristics  $U/U_{med}$

In Figure 23, the characteristics of the flow are presented on the graphic. It can be seen clearly the difference between the inner and the outer jet  $U_{mean}$  velocities. At the

entrance of the test section, there is the initial merging zone wherein the inner and the outer streams enter the mixing test section with different uniform axial velocities. As long as the flow progresses, the velocities decrease. The outer jet (with bigger velocity) spreads towards the center and the inner potential core starts to decrease. The entrainment effect is observed on the green region where the inner jet is accelerated while the outer jet decreases his velocity for  $Y/b=1$ .

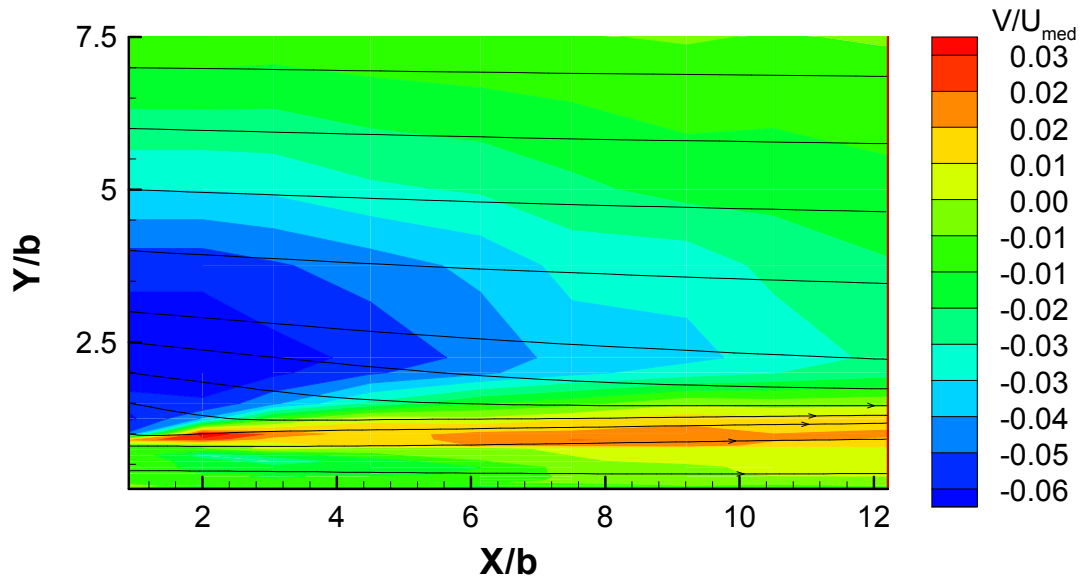


Fig. 24 Isolines of mean velocity characteristics  $V/U_{med}$ .

In Figure 24, the characteristics of the  $V/U_{med}$  are observed. Starting the analysis by the entrance of the flow, the figure shows that at the level of the splitter plate ( $Y/b=1$ ) for  $X/b=2$ , there is a maximum  $V/U_{med}=0.3$ . This is probably due to the trailing edge of the splitter plate. Upward the splitter plate,  $V/U_{med}$  has negative values because the vertical component of the velocity wasn't completely eliminated on the divergent. As the flow progresses, the maximum value for  $V/U_{med}$  is always on the region where the inner and outer jet mixed them and where the shear stresses are bigger. For a velocity ratio of 2, there is no recirculation zone.

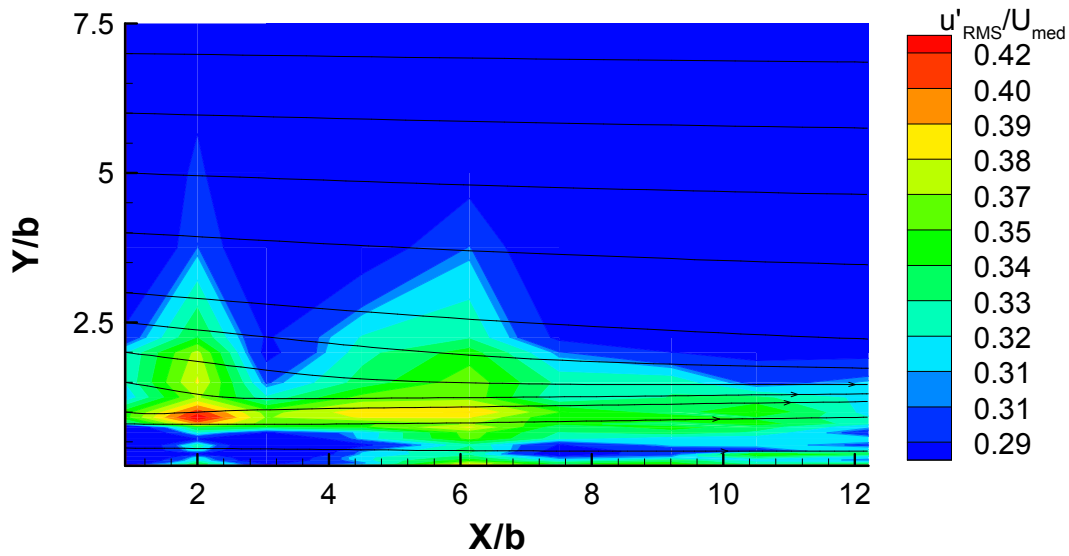


Fig. 25 Isolines of turbulent characteristics  $u'_{RMS}/U_{med}$ .

On Figure 25, it is shown the turbulent characteristics for  $u'_{RMS}/U_{med}$ . At the entrance of the flow, the biggest value for  $u'_{RMS}/U_{med}$  is found for  $Y/b=1$  where the splitter plate is positioned. The splitter plate causes a wake effect on the flow. As long as the flow progresses, it is shown that the turbulence intensity increases on the outer jet due to the vertical plates from the wind tunnel. That causes a faster mixing and the outer jet is deflected into the center. The shear layer between each pair of jets is a region of intense velocity fluctuations.

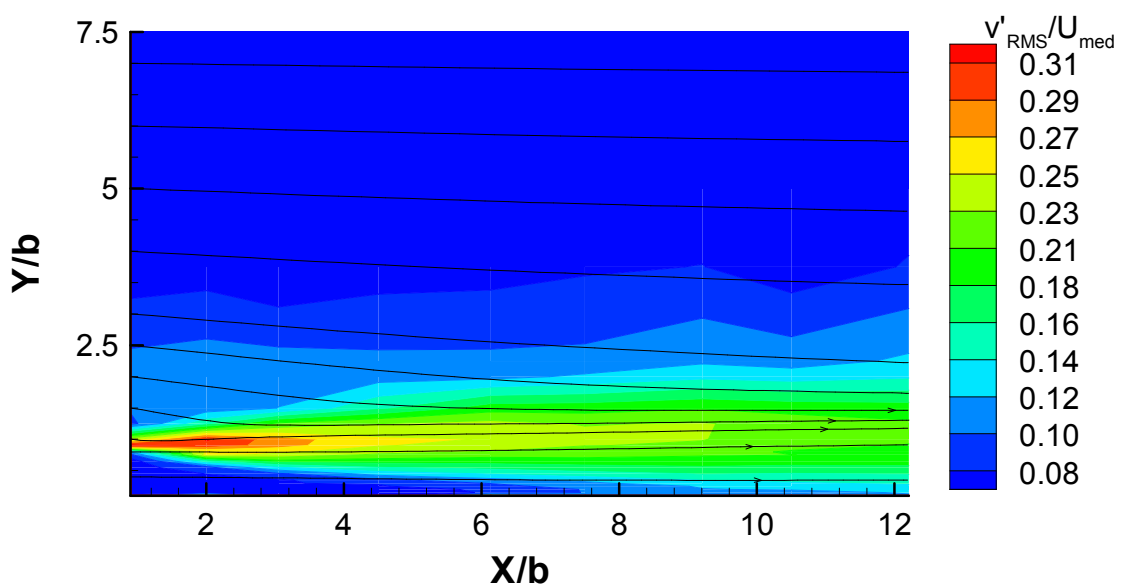


Fig. 26 Isolines of mean velocity characteristics  $v'_{RMS}/U_{med}$ .



In Figure 26, the turbulent characteristics for  $v'_{\text{RMS}}/U_{\text{med}}$  are shown.. It is observed as on Figure 25, that there is the same wake effect cause by the splitter plate. This maximum value reaches 0.31 on this zone. As the flow progresses, the maximum turbulence intensity is find on the region where the two flows interact. The shear layer between each pair of jets is a region of intense velocity fluctuations.

Dziomba and Fiedler [21], showed that when the thickness of the splitter plate separating two streams of different velocity is increased, the Kelvin-Helmholtz instability of the shear layer is progressively replaced by a regular alternate shedding of vortices in the wake. Turbulent intensities are 30% of the mean mass flow velocity ( $U_{\text{mean}}$ ) that correspond to a ratio between the outer and inner jets of  $\theta=1.5$ . High levels of turbulent mixing inhibit the flow reversal that has been detected for higher values of  $\lambda$ .

### 3.5 Relations with the Shear layer

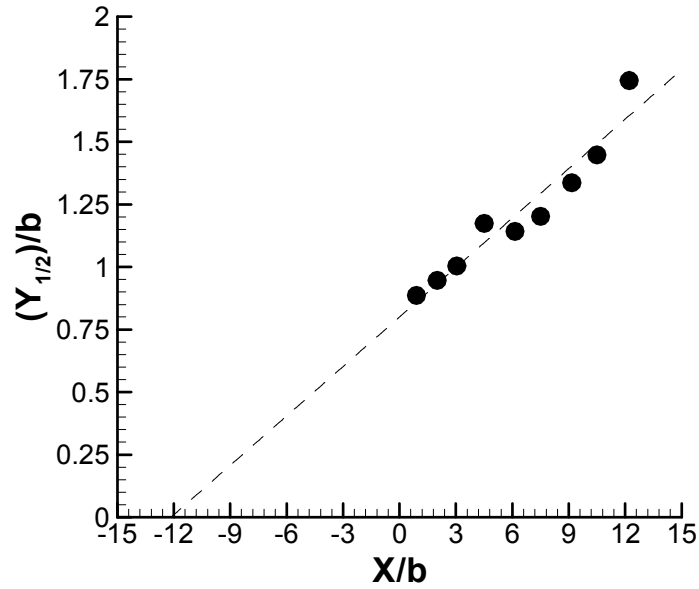


Fig. 27 Spreading rate of the outer flow

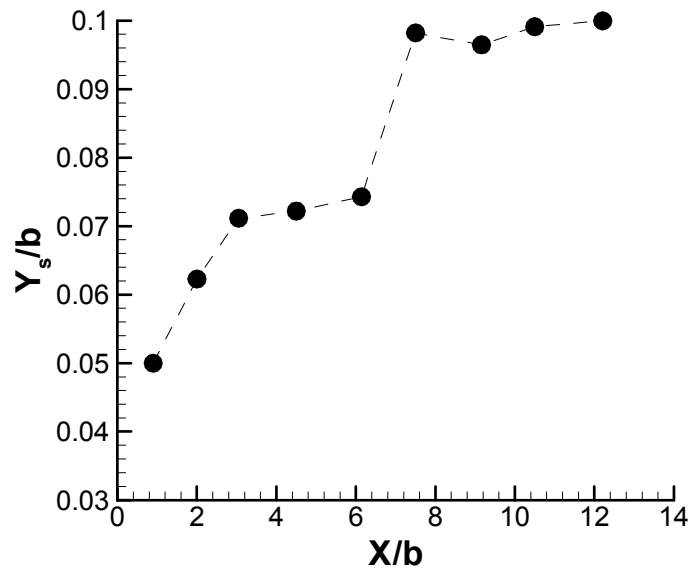
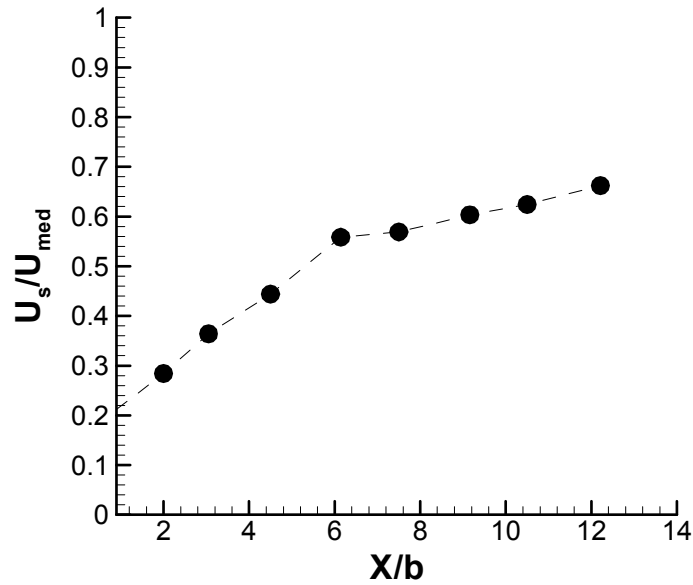


Fig. 28 Variation of the location of the shear layer interface with distance to the jets exit.



**Fig. 29** Variation of the mean horizontal velocity component of the shear layer

In Figure 27, 28 and 29, it can be observed that the outer flow is deflected to the center, because the distance of  $Y/b$  to the ground is increasing and the spreading rate of the outer flow is about  $6^\circ$ . The mean horizontal velocity component on the shear layer increases over  $X$  but not linearly. In Figure 27, it's shown that the variation of the location of the shear layer interface with distance to the jets exit is not linear. This is due to the effect of the confinement.

## CHAPTER 4

### 4 Conclusions

Turbulent mixing of two parallel streams is affected by confinement, velocity ratio, and turbulent intensity. The objective of this work was to study the effect of the initial levels of turbulence of each coaxial jet in the process of turbulent mixing for diameter ratios less than 2, which is the case of very low bypass turbofan engines. The use of convenient turbulent intensity ratios between the inner and outer flow should be a most effective tool to control the turbulent mixing between the inner and outer flow ( $\theta$ ). The aim of the present work was to study the effect of  $\theta$  on the flow development and to identify the associated regimes, and in particular the production of a flow reversal in the central zone near the jets exit. To isolate the characteristic radial effects of a cylindrical geometry a bi-dimensional configurations was adopted.

The presence of a significant wake effect in the initial merging zone of the inner mixing layer was assured by mean velocity profiles and the fluctuating velocity components. In the near region, a peak of turbulent characteristic of the vortex shedding occurred behind the splitter plate. For  $X/b$  greater than typically 4.5, the effect of the wake disappeared and was overcome by the mixing layer influence.

The turbulence levels inside both the inner and outer mixing layer were of quite comparable magnitudes while it was more common for the outer mixing layer to be higher turbulence level than the inner mixing layer. The mean velocity profiles clearly showed the wake effect of the splitter plate. As long as the flow progressed, on the visualization the potential core in the inner stream disappears.

During this study, no recirculation was identified for a velocity ratio of 2. The shear layer between each pair of jets was a region of intense velocity fluctuations and the high levels of turbulent mixing inhibited the flow reversal that has been detected for higher values of  $\lambda$ .

The self-preserving condition was not been reached within the domain of the present measurements for the velocity ratio in consideration.

Regarding future work, it is necessary to made experimental studies for higher velocity ratios considering high levels of turbulence intensities to simulate the recirculation bubble and to identify and quantify the parameters that influences this phenomenon. The study of other parameter like the shear stresses on the mixing area could be interesting to analyze energy balance and vorticity for further comparison with numerical studies.

## References:

- [1] M.R. Ahmed e S.D. Sharma “Effect of velocity ratio on the turbulent mixing of confined, co-axial jets”, *Experimental Thermal and Fluid Science* 22, pp 19-33, 2000.
- [2] E. Razinsky, J.A. Brighton, “Confined jet mixing for non-separating conditions”, *ASME J. Basic Eng.* 93 (3) (1971) 333-347.
- [3] Y.V.G. Acharya, ”Momentum Transfer and Heat Diffusion in the Mixing of Co-axial Turbulent Jets Surrounded by a Pipe, Vliegtuig bouwku-ndig Ingenieur Geboren Te Mysore, Uitgeverij Excelsior, India, 1954.
- [4] S. Mikhail,” Mixing of co-axial streams inside a closed conduit”, *J. Mech. Eng. Sci.* 2 (1) (1960) 59-68.
- [5] K. Albayrak, O.C. Eralp, B. Celen, “An investigation on the mixing region of co-axial jets”, *Modelling, Simulation Control,Part B* 33 (2) (1990) 49-64.
- [6] M.M. Gibson, “Hydrodynamics of confined co-axial jets”, *Encyclopedia Fluid Mech.* 2 (1986) 367-390.
- [7] M.R. Ahmed, “Experimental investigation on turbulent mixing in co-axial, confined jets with low annular to core area ratio”, Ph.D.Thesis, Department of Aerospace Engineering, Indian Institute of Technology, Bombay, 1997.
- [8] T.S. Zawacki, H. Weinstein, “Experimental investigation of turbulence in the mixing region between co-axial streams”, *NASA CR-959* (1968).
- [9] T. Rozenman, H. Weinstein, “Recirculation patterns in the initial region of co-axial jets”, *NASA CR-1595* (1970).
- [10] D. Durao, J.H. Whitelaw, “Turbulent mixing in the developing region of coaxial jets”, *Trans ASME, J. Fluids Engng* 95 (1973) 467–473.

- 
- [11] N.W.M. Ko, H. Au, "Initial region of subsonic coaxial jets of high mean velocity ratio", *Trans ASME, J. Fluids Engng* 103 (1981) 335–338.
- [12] Warda HA, Kassab SZ, Elshorbagy KA, Elsaadawy EA (2001) "Influence of the magnitude of the two initial velocities on the flow field of a coaxial turbulent jet", *Flow Meas Instrum* 12:29–35
- [13] R. Curtet and F.P. Ricou, "On the tendency of self-preservation in jets". *ASME J. Basic Eng.* 86 4 (1964), pp. 765–776.
- [14] L.E. Fink, "Influence of external turbulence on mixing of axisymmetric co-axial jets", in: *Proceedings of the First Symposium on Turbulent Shear Flows*, 2.11–2.21 (1977)
- [15] S.N. Singh, D.P. Agarwal, R.C. Malhotra, "Mean velocity distribution of contra-swirling co-axial confined jets", *Exp. Fluids* 7 (2) (1989) 501-504.
- [16] R.M.C. So, S.A. Ahmed, H.C. Mongia, "Jet characteristics in confined swirling flows", *Exp. Fluids* 3 (1) (1985) 221-230.
- [17] Buresti G, Talamelli A, Petagna P (1994) "Experimental characterization of the velocity field of a coaxial jet configuration" *Exp Therm Fluid Sci* 9:135–146
- [18] Warda HA, Kassab SZ, Elshorbagy KA, Elsaadawy EA (1999) "An experimental investigation of the near field region of free turbulent round central and annular jet" *Flow Meas Instrum* 10:1–14
- [19] R.V. Kamath, Numerical analysis and experimental investigation of ejectors, Ph.D. Thesis, Department of Aerospace Engg., Indian Institute of Technology, Bombay (1996).
- [20] R. Matsumoto, K. Kimoto, N. Tsuchimoto, A study on double concentric jets, *Bulletin of JSME* 16 (93) (1973) 529-540.
- [21] B. Dziomba, H.E. Fiedler, Effect of initial conditions on two dimensional free shear layers, *J. Fluid Mech.* 152 (1985) 419±442.

- [22] Nikitopoulos, D. E., J. W. Bitting, and Gogineni, “Comparison of initially turbulent, low-velocity circular and square coaxial jets.” *AIAA Journal*, 2003. 41(2):pp 230-239
- [23] Bitting, J. W. Et al., “Visualization and two-colour DPIV measurements of flow in circular and square coaxial nozzles.” *Experiments in Fluids*, 2001. 31(1), pp 1-12
- [24] Balarac, G. And M. Si-Ameur, “Mixing and coherent vortices in turbulent coaxial jets” ,*Comptes Rendus Mecanique*, 2005. 333(8), pp 622-627
- [25] Villiermaux, E. 1998<sup>a</sup> “Mixing and Spray formation in coaxial jets”. *L. Prop. Power*14, 807-817.
- [26] Zhdanov, V.; Kornev, N; Hassel,E.; Chorny, Andrei; “Mixing of confined coaxial flows”,*International Journal of Heat and Mass Transfer* 49 (2006)
- [27] H. Rehab, E. Villiermaux, and E. J. Hopfinger, “Flow regimes of large velocity-ratio coaxial jets,” *J. Fluid Mech.* 345, 357 (1997)
- [28] Revuelta A., Sánchez A. L. and Liñan A., “Confined axissymmetric laminar jets with large expansion ratios”, *Journal of Fluid Mechanics* (2002).
- [29] Talamelli, A., Gavarini, I., “Linear instability characteristics of incompressible coaxial jets” *Flow Turbulence Combust* (2006) 76:221–240
- [30] Dahm,W. J. A. & Dimotakis, P.E. 1987 “Measurements of entrainment and mixing in turbulent jets”. *AIAA J.*25, 1216-1223.
- [31] M. R. Ahmed & S. D. Sharma, “Turbulent mixing enhancement with a 20° chute mixer”, Elsevier Science, New York, *Experimental thermal and fluid science*, 2006, vol.30, no3,pp.161-174
- [32] Champagne, F.H & Wygnanski, I.J. “An experimental investigation of coaxial turbulent jets”*J. Heat Mass Transfer.*4, 1445-1466
- [33] Ribeiro MM, Whitelaw JH (1980) “Coaxial jets with and without Swirl”. *J Fluid Mech.* 96(part 4):769–795



- [34] Ribeiro MM (1972) “Turbulent mixing of coaxial jets”, Imp College of Sc and Tech University of London
- [35] W. J. A. Dahm, C. E. Frieler, and G. Tryggvason, “Vortex structure and dynamics in the near field of a coaxial jet,” J. Fluid Mech. 241, 371 (1992)
- [36] Sadr, R., Klewicki, J.C., “An experimental investigation of the near-field flow development in coaxial jets”, Physics of Fluids, Vol 15, n°5 (2003)
- [37] M. Lima J. Palma, “Mixing in Coaxial Confined Jets of large Velocity Ratio”
- [38] Balarac, G. & Métais, O., “The near field of coaxial jets: A numerical study”, Physics of Fluids 17, 065102 (2005)
- [39] Barata, J., Neves F., Silva A., “Estudo Numérico do Efeito do Nivel de Turbulencia inicial na mistura de jactos coaxiais confinados – Parte I”, Universidade da Beira Interior
- [40] Barata, J., Neves F., Silva A., “Estudo Numerico do Efeito do Nivel de Turbulencia inicial na mistura de jactos coaxiais confinados – Parte II”, Universidade da Beira Interior
- [41] M.M. Ribeiro, J.H. Whitelaw, “Turbulent mixing of coaxial jets with particular reference to the near-exit region”, Trans ASME, J. Fluids Eng. 98 (1976) 284–291.
- [42] R.D. Mehta, “The Aerodynamic Design of Blower Tunnels with Wide-Angle Diffusers”, Department of Aeronautics, Imperial College, London.
- [43] R.D. Mehta and P. Bradshaw, “ Design rules for small low speed wind tunnels”, The Aeronautical Journal of the Royal Aeronautical Society, November 1979.
- [44] Barata, J.M.M., Durão, D.F.G. (2005) “Laser-Doppler Measurements of a Highly Curved Flow”. AIAA Journal, Vol. 43, No.12:2652-2655.
- [45] Yanta, Z., Smith, R.A. “Measurements of Turbulent-Transport Properties with Laser-Doppler Velocimeter.” AIAA Paper 73-0169, 11<sup>th</sup> Aerospace Sciences Meeting, Washington.

